

PISTON RING FRICTION

by

CLARENCE TEH-CHING CHANG

B.S.E., University of Pennsylvania
(1980)

SUBMITTED TO THE DEPARTMENT OF
MECHANICAL ENGINEERING IN PARTIAL
FULFILLMENT OF THE
REQUIREMENTS FOR THE
DEGREE OF

MASTER OF SCIENCE IN
MECHANICAL ENGINEERING

at the

MASSACHUSETTS INSTITUTE OF TECHNOLOGY

June 1982

© MASSACHUSETTS INSTITUTE OF TECHNOLOGY 1982

Signature of Author _____

Department of Mechanical Engineering
April 28, 1982

Certified by _____

David P. Hoult
Thesis Supervisor

Accepted by _____

Archives

Warren G. Rohsenow
Chairman, Departmental Graduate Committee

MASSACHUSETTS INSTITUTE
OF TECHNOLOGY

JUL 30 1982

PISTON RING FRICTION

by

Clarence T. Chang

Submitted to the Department of Mechanical Engineering on Apr. 28, 1982 in partial fulfillment of the requirements for the Degree of Master of Science in Mechanical Engineering.

ABSTRACT

Hydrodynamic piston ring lubrication and friction phenomenon, locally, may be characterized by five dimensionless parameters. (It is not necessary to take into consideration of all the terms of the modelling equations.) Three of these are consisted of geometrical and physical characteristics of the piston ring; the other two are related to the lubricant and piston kinematic of engine operation.

Two computer programs are discussed here: ESMOD and COMSEC. They approximate the lubrication film shape by an effective slope and a composite secant respectively.

The numerical simulation results indicated that high oil viscosity and high engine speed are the largest contributors to friction loss; ring elastic pressure influenced friction loss very weakly. Also, the simulation indicated that oil control rings (OCR) may have inherently higher friction than the compression ring because the OCR has a higher cross-sectional aspect ratio.

Thesis Supervisor: Dr. David P. Hoult

Title: Senior Research Associate
Department of Mechanical Engineering

Abide in Me, and I in you. As the branch can not bear fruit of itself, unless it abides in the vine, so neither can you, unless you abide in Me.

I am the vine; you are the branches; he who abides in me, and I in him, he bears much fruit; for apart from Me, you can do nothing.

Jesus
John 15:3,4

ACKNOWLEDGMENTS

I wish to express my appreciation to Professor David P. Hoult for his guidance and encouragement during the course of this research. Many thanks also, to Mr. Frank O'Brien for the suggestions and many insights into the physics of the research subject.

Many thanks to my housemate Michael Gallagher for the final grammar editing. Thanks to my fellow students in the Sloan Automotive Lab. for the precious informations and suggestions. Also, thanks to Barbara Langford for the help with the word processor.

My gratitude to Christ Jesus, who gave me his "peace that surpasses all understanding," as he has promised, in the many dark days of my life.

This work was supported by U. S. Department of Energy.

Clarence T. Chang
Cambridge, Massachusetts

CONTENTS

Abstract

Acknowledgment

Contents

Nomenclature

1. Introduction
 - 1.1 Background
 - 1.2 Purpose
 - 1.3 Assumptions
2. General Conceptual Model
 - 2.1 Ring profile and geometry
 - 2.2 Lubrication model
 - 2.2.1 Film lubrication
 - 2.2.2 Friction loss from fluid shear
 - 2.3 Ring dynamics
 - 2.3.1 Modes
 - 2.3.2 Ring as a free body
 - 2.4 Governing equation list
 - 2.5 Ring rigidity
3. Non-dimensionalization of equations
 - 3.1 Characteristic variables
 - 3.2 Dimensionless equations
 - 3.3 Dimensionless parameter list and term size
4. Quasi-Static Models and Dynamic Simulation
 - 4.1 Dynamic simulation evaluation
 - 4.2 Analytical approximations
 - 4.3 Simplifications
 - 4.3.1 Simplified equations
 - 4.3.2 Simplified dimensionless parameter list
5. Effective Slope Model (ES)
 - 5.1 Geometry and organization
 - 5.2 Computational organization
 - 5.3 Input/output
6. Composite Secant Model (CS)
 - 6.1 Geometry and pressure field
 - 6.2 Boundry conditions
 - 6.3 Oil forces and moments
 - 6.4 Total forces and moments
 - 6.5 Computational organization
 - 6.6 Input/output

7. Results and Discussion
 - 7.1 Computational result
 - 7.2 Discussions
 - 7.3 State variable variations

8. Conclusions

References

Appendicies

- Appendix A1: Effective Slope Model Program (ESMOD) Listing
- Appendix A2: ESMOD flow chart
- Appendix A3: DATA4 Input format sample
- Appendix A4: DATA5 Output format sample
- Appendix B1: Composite Secant Model Program (COMSEC) Listing
- Appendix B2: COMSEC flow chart
- Appendix B3: DATA7 input format sample
- Appendix B4: DATA8 output format sample

NOMENCLATURE

A	Ring cross-sectional area
B	Ring radial width
C_{deg}	Spring constant of ring deflection
C_{tw}	Spring constant of ring twist
C_{μ}	Nominal coefficient of friction
D_p	Pivot point distance from the ring groove edge
E	Modulus of elasticity of ring
F	The force that the piston land exerts on the ring
F_{μ}	The axial film friction force
F_{μ}'	Normalized friction
I	Ring cross-section moment of inertia for radial deflection
J	Polar moment of inertia of ring cross-section
h	Local film height under the ring, $h(x,t)$
h_a	Axial distance between the top of the ring and the topland
\bar{h}	Characteristic film height
h_p	Ring local contour height
h_r	Ring reference film height
h^i	Normalized local film height
h_a'	Normalized axial distance in the ring groove
h_p'	Ring local contour height
h_r'	Normalized ring reference film height
P_e	Ring elastic pressure (pre-stressed)
P_0	Pressure below the ring
P_1	Pressure above the ring
ΔP_1 or	
ΔP	Pressure difference across the ring
P_0'	Normalized pressure below the ring
P_1'	Normalized pressure above the ring
$\Delta P_1'$ or	
$\Delta P'$	Normalized pressure difference
R	Crank radius
R_{cyl}	Cylinder bore radius
t	Time
U	Axial piston speed
U'	Normalized piston speed
V	Circumferential ring speed
W	Ring axial width
x	Axial coordinate between ring and wall
x'	Normalized axial coordinate under the ring
y	Circumferential coordinate under the ring
Y	Piston axial location
\ddot{Y}	Piston acceleration
\ddot{Y}'	Normalized piston acceleration
α	Ring tilt angle
α_m	Maximum ring tilt angle
$\bar{\alpha}$	Characteristic ring tilt angle
α'	Normalized ring tilt angle
α_0'	Normalized maximum ring tilt angle
η	Dynamic viscosity of oil
ρ	Ring density

ρ_f Oil density
 ω Frequency of natural vibration for ring twist
 θ Crank angle

EFFECTIVE SLOPE MODEL NOMENCLATURE

K Combination stante variable
 M_B Oil pressure moment from the trailing edge of ring
 due to pressure drop
 X^* Center of oil film pressure from the trailing edge
 \bar{X}^* Normalized Center of oil film pressure
 ϕ Effective slope angle
 ϕ' Normalized effective slope angle

COMPOSITE SECANT MODEL NOMENCLATURE

C_1 Constant of integration
 C_2 Constant of integration
 L_1 Width of ring above ring profile crest
 L_2 Width of ring below ring profile crest
 Δh_1 Ring profile height at top of ring
 Δh_2 Ring profile height at bottom of ring
 θ Transformed coordinate in the film
 $\bar{\theta}$ Constant of integration
 ζ_1 Transformed coordinate at the top edge of the ring
 ζ_2 Transformed coordinate at the bottom edge of the ring

CHAPTER 1

Introduction

1.1 Background

The internal combustion engine is one of the most commonly used means of power generation, especially in transportation. It is used because of its simplicity, durability, and efficiency. In order to contain the working fluid within the cylinder, piston rings are used to seal the annulus region between piston and the cylinder wall.

This arrangement, however efficient for sealing, has created high frictional losses. In fact, some twelve percent of the gross energy output of the engine is lost due to the friction between the ring and the piston skirt. This raises several important questions: Is it possible to reduce these losses? What are the most important parameters that effect the friction mechanism?

Piston rings have a long history. Piston ring lubrication was not understood until Reynolds developed the hydrodynamic lubrication theory around 1904. For the next fifty years, the performance of some specific ring, oil, and piston combinations were established empirically. But the local mechanism that governed the friction was not well defined.

Today, There are several analytical models that are available. Furuhashi has developed a two degrees of freedom model predicting the trend of the friction. This predicted value, however, is substantially smaller than the experimental value. This is not surprising, since the conditions surrounding the friction are idealized in the model.

Rangert (1974) of Chalmers University of Technology, Sweden, has developed a friction model to examine lubrication oil consumption. With three degrees of freedom, (including ring twisting), however, the scale of his consumption calculation was very large, and the treatment of friction was minimal.

This thesis summarizes the results of a research effort based mainly on Rangert's model.

1.2 Purpose

The aim of this research is to analytically study piston ring lubrication. First, the dimensionless parameters that characterize the operation of a piston ring and its friction were identified. The sizes of the various dimensionless parameters determine their relative influence on the behavior of the ring.

Next, an analytical model describing the dynamics surrounding the ring's performance was developed. Using this analytical model in numerical simulation, the operational behavior of a piston ring was predicted relatively quickly. The film thickness, ring twist

angle, and friction of the piston ring were computed in the numerical simulation.

1.3 Assumptions

There are a number of assumptions that are made in this model that are necessary to isolate local piston ring friction.

One of the single largest causes of friction in an internal combustion (IC) engine is the side thrust force exerted by the crank rod on the piston. This force is then transmitted to the cylinder wall on the thrust face, resulting in noticeable wear on the cylinder wall near the top dead center (TDC) position of the first ring. Reducing the mass of the components by using lighter materials and smaller parts can minimize this loss by reducing the side thrust force. Since this thesis is primarily interested in the local interaction between the ring, the piston and the wall, the side thrust force is neglected.

How much the ring deflects locally determines the local elastic pressure that it exerts on the wall. The piston ring normally employed has a gap in its circumference. The ring is much wider in its relaxed state. Upon installation, it is forced into the cylinder of the piston, which is smaller in diameter than the diameter of the relaxed ring. This means that the ring has to deflect inward from the relaxed position. This work assumes that this elastic pressure is a constant value azimuthally. In other words, this model assumes that the ring behaves like a washer: it con-

tracts and expands equally around the circumference.

There is cause for concern, however, since the deflection spring constant for the washer is much larger than the actual constant, (on the order of 100 times stiffer) and the deflection constant for a cantilever beamed ring is much too soft. So, in modelling the ring, the constant is assumed to be the clamping force at the ring gap divided by the projected ring contact area (the cylinder bore diameter times ring axial width).

The lubrication oil film breaks down near the TDC position on the compression stroke. One of the causes is that the oil surface tension increases with temperature and the oil tends to congregate into droplets. This was observed by Wing and Saunder in 1975. This model assumes that the ring always rides on a full fluid film. The surface tension effect is beyond the scope of study for this thesis.

Exactly how a piston ring is supported in the ring groove is unclear, although there are several theories in existence. One of the difficulties is that the desired tolerances are beyond the control of our manufacturing abilities.) This model adapts Rangert's model that the ring rests on a single point with a rolling contact on the topland or the bottomland in the ring groove. The angle of ring tilt determines the contact point. The equations below describe the distance of the pivot point from the cylinder wall.

Ring at bottomland: $D_p = (1 - \alpha'/\alpha_0')(B/2)$

Ring at topland: $D_p = (1 + \alpha'/\alpha_0')(B/2)$

$$\alpha_0' = \alpha_m / \bar{\alpha}$$

$\bar{\alpha}$ is the characteristic ring twist angle

α_m is the maximum ring tilt angle

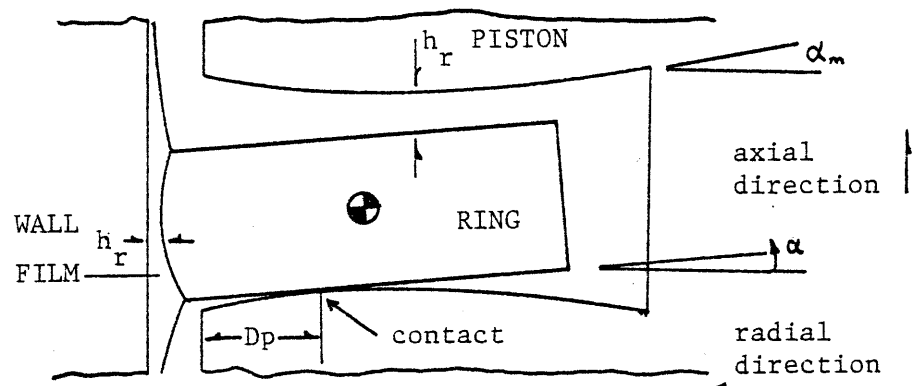


Fig. 1.4-1 Ring pivot position

Since there is a single point of contact, this model assumes that the contact point seals the pressure on one side from the other, so that there is a step change in the pressure across this contact point.

Normally either the gas pressure or piston acceleration holds the ring against one of the lands. Since there is oil in between the ring and the land, and radial movements by the ring create friction between the ring and the land. However, since the radial motion of the ring is smaller than its motions in other directions this friction is assumed to be small compared with other forces, and is neglected.

Finally, the physical properties of the oil, such as viscosity, and density are considered constant. The physical properties of the ring, such as density and modulus of elasticity are considered constant.

In addition, this model assumes adequate oil feed such that there is always a full film of oil under the ring.

CHAPTER 2

Generalized Conceptual Model

With the above mentioned assumptions in mind, the piston ring has three (3) degrees of freedom, each associated with one state variable. The piston ring moves radially closer or further from the cylinder wall, a distance denoted by h_r . This is also the reference film height. In addition, the ring moves axially. Its position is marked by h_a , the axial location. Lastly, the ring twists in the groove in order to create the proper flow channel shape. This inclination angle is denoted α . (The positive direction is for the inside of the ring to move toward the combustion side. See Figure 1.4-1)

2.1 Ring Profile Geometry

Several types of rings are on the market presently. This work shall focus on the ring with rectangular cross section.

The dimensions of the ring are denoted as follows:

Axial width	:	W
Radial width	:	B
Cylinder bore radius	:	R_{cyl}

The density and the elastic modulus are homogenously

distributed in the ring.

It is necessary to assume a rigid ring surface. The top and bottom surfaces are flat, and the front surface is curved. This curved surface has its peak at the geometric center of the ring surface, and the profile is roughly symmetrical about this point. The shape is largely determined by the wearing process, since it is below manufacturing tolerances. The wear-in height is in the order of one to five micrometers, and it is roughly $\Delta h = B/1000$.

The ring surface roughness is usually about 0.5 micrometer for a worn-in ring and up to four micrometers for a polished new ring.

2.2 Lubrication Model

2.2.1 Film Lubrication

There is a thin film of lubrication oil on the surface of the cylinder wall, and the piston rings ride on this thin film. Although it is only between one to ten micrometers thick, it is sufficient to keep the protrusions of the ring surface from contacting the wall. (At various regions of the operation, boundary lubrication dominates.) The pressure build up in the oil film separates the two surfaces when they move relative to each other. This pressure build up is described by Reynold's Equation

$$\frac{\partial}{\partial x} \left(h^3 \frac{\partial P}{\partial x} \right) + \frac{\partial}{\partial y} \left(h^3 \frac{\partial P}{\partial y} \right) = 6U\eta \frac{\partial h}{\partial x} + 6V\eta \frac{\partial h}{\partial y} + 12\eta \frac{\partial h}{\partial t} \quad (2.2-1)$$

in which U and V are the velocities in the x and y directions respectively. Local film pressure and thickness are P and h. The axial coordinate of oil film under the ring is x.

Since this work assumes that the azimuthal conditions are symmetrical, then the derivatives with respect to y direction drops out of the equation, and leaves

$$\frac{\partial}{\partial x} \left(h^3 \frac{\partial P}{\partial x} \right) = 6U\eta \frac{\partial h}{\partial x} + 12\eta \frac{\partial h}{\partial t} \quad (2.2-2)$$

The first term on the right hand side describes the pressure change due to a convergent or divergent passage way. This is the dominant effect throughout most of the cycle except when the piston is near the end of the stroke where its velocity is relatively low.

The second term produces pressure in the flow channel by virtue of the collapse of the channel. This is easily visualized when a flat sheet of paper settles on a flat surface: the paper floats for a while, supported by the pressure under it until the trapped air is gone. This squeezing effect is most dominant at the end of the stroke where the piston velocity is very low.

In order to produce pressure in the oil film, the film thickness under the ring must change. We represents the film height as

$$h(x,t) = h_p(x) + h_r(t) + \alpha(t) \cdot x \quad (2.2-3)$$

where $h(x,t)$ is the local film height. The ring profile height is $h_p(x)$. The ring reference distance is $h_r(t)$. And the ring inclination angle is $\alpha(t)$. Change in any one of these components will change the pressure distribution.

2.2.2 Friction Loss from Fluid Shear

From classical slit flow theory, the shear between two parallel plates is

$$\text{Shear} = \frac{h}{2} \frac{\partial P}{\partial x} - \frac{\eta U}{h} \quad (2.2-4)$$

Integrating the shear under the ring surface produces the total ring friction.

2.3 Ring Dynamics

2.3.1 Ring Modes

In the piston, the piston ring fits loosely in the ring groove. Usually, there is room in the back of the ring, and there is room axially. This means that the ring may move axially in the ring groove, from top-land to bottom-land, depending upon the operating conditions. From the nature of this model and the Namazian calculation (1981), the actual transition interval is in the order of a few degrees of crank angle. Therefore, it is safe to assume that the ring rests most of the time on either the top-land or the bottom-land. See Figure 2.2-1.

Secondly, both Rangert (1974) and this model have shown that the diagonal corners of the ring do not contact the top and bottom surfaces of the ring groove simultaneously. This means that there is always a single point contact between the piston and the ring that acts as the pivot point.

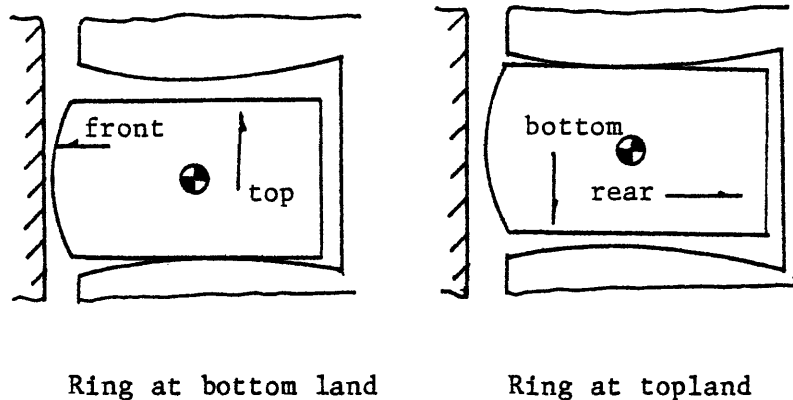


Fig. 2.2-1 Ring modes at bottom and top land

2.3.2 Ring as a Free Body

The ring is a free body influenced by outside forces.

On the front surface, there is the normal oil pressure distributed over the axial width. This produces both a normal force as well as a moment on the ring surface. In addition, fluid shear on the face produces drag. Consequently, it produces a moment about the pivot point.

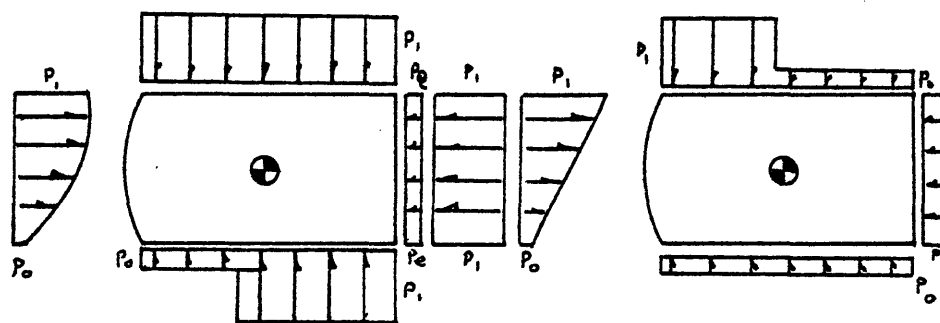
If the ring is resting on the bottomland, then the passage above it offer little flow resistance so that the pressure above and behind the ring are assumed to be the chamber pressure above, such as the combustion pressure. The pressure below, however, has

a step, since the contact point seals the pressure across it.

When the ring is resting on the topland, the pressure step is on the top surface; the pressure behind and below the ring is the same as the pressure in the chamber below, such as the crank case.

The elastic properties of the ring also exerts an effective elastic pressure on the ring in the radial direction. In addition, the torsional rigidity of the ring creates a moment when the inclination of the ring is not in its natural state.

Lastly, the inertial properties of the ring exerts a d'Alembert force axially on the ring, since it is moving in the accelerated frame of the piston. Because the contact point of the ring with the piston shifts with the ring inclination, it may be askew with respect to the center of mass of the ring. Therefore, there is a moment at the pivot point.



Ring at bottomland

Ring at topland

Fig. 2.3-1 Pressure distribution about ring

2.4 Governing Equation List

Reynold's Equation of Viscous Flow

$$\frac{\partial}{\partial x} \left(\eta^3 \frac{\partial P}{\partial x} \right) - 6U\eta \frac{\partial h}{\partial x} - 12\eta \frac{\partial h}{\partial t} = 0 \quad (2.4-1)$$

The left hand side of the following equations are ring reactions.

Moment Balance

$$\begin{aligned} \rho J \frac{d^2 \alpha}{dt^2} &= (P_0 - P_1) \frac{D_p^2}{2} - \frac{EBW^3}{12 R_{cyl}^2} \alpha \\ &- \int_0^W (P(x) - P_0)(W-x) dx + P_e W^2 / 2 + \frac{5EW^2 B^3}{6\pi^4 R_{cyl}^4} h_r \\ &- \int_0^W \frac{h}{2} \frac{\partial P}{\partial x} D_p dx + \int_0^W \frac{U \eta D_p}{h} dx - \rho A \ddot{Y} \left(\frac{B}{2} - D_p \right) \end{aligned} \quad (2.4-2)$$

first term: pressure moment from step pressure

second term: torsional rigidity moment (elastic)

third term: difference of oil pressure and gas pressure

fourth term: elastic pressure

fifth term: elastic force moment

sixth and

seventh term: shear force moment

eighth term: inertial force moment

Radial force

$$\rho A \frac{d^2 h_r}{dt^2} = \int_0^W (P(x) - P_0) dx - P_e W - \frac{20 EI}{\pi R_{cyl}^4} h_r \quad (2.4-3)$$

first term: difference of oil lift force and back gas pressure force

second term: elastic force (pre-stressed)

third term: elastic force

Axial force

$$\rho A \frac{d^2 h_a}{dt^2} = \int_0^W (P_0 - P_1) D_p + \int_0^W \left(-\frac{h}{2} \frac{\partial P}{\partial x} - \eta \frac{U}{h} \right) dx - \rho A \ddot{Y} + F \quad (2.4-4)$$

first term: stepped gas pressure

second term: shear

third term: inertia

fourth term: from top or bottom of ring groove

2.5 Ring Rigidity

Using classical applied mechanics formula for a cantilever beam, we can formulate the bending force required to bend a beam a radial distance. However, since this deflection spring constant varies about the periphery of the piston axis, an averaged value is presented below:

$$F_{ela} = -C_{def} \cdot h_r ; C_{def} = \frac{20 EI}{\pi R_{cyl}^4} \quad (2.5-1)$$

Where I is the ring crosssectional moment of inertia.

Similarly, for torsional load, there is a restoring moment in the ring due to its being twisted. Rangert gave

$$M_{ela} = -C_{tw} \cdot \alpha ; C_{tw} = \frac{EBW^3}{12 R_{cyl}^2} \quad (2.5-2)$$

CHAPTER 3

Non-dimensionization of Governing Equations

3.1 Characteristic Variables

In order to compare the operations of various rings, it is necessary to reduce the physical problem into a mathematical problem. The non-dimensionalization of this can shed much light on the phenomenon. We formulate the following characteristic variables to normalize the equations:

The coordinates under the ring is normalized against the ring width.

$$X' = X / W ; dx' = dX / W$$

Time is normalized against the characteristic time for the average piston speed to travel the crank radius.

$$t' = t (\bar{U} / R) ; dt' = dt (\bar{U} / R)$$

The pressure is normalized against the ring elastic (pre-stressed) pressure.

$$P' = P(x,t)/P_e ; P_1' = P_1/P_e ; P_0' = P_0/P_e$$

The film height components are normalized against the characteristic film thickness, \bar{h} , which is taken to be the the profile height, Δh

$$h_r' = h_r / \bar{h} ; h_p' = h_p / \bar{h} ; h_a' = h_a / \bar{h}$$

The ring inclination angle is normalized against the

characteristic ring inclination angle, $\bar{\alpha}$.

$$\alpha' = \alpha / \bar{\alpha} ; \text{ where } \bar{\alpha} = 12P_e \bar{h}^3 / (\bar{U} \eta W^2)$$

Piston speed is normalized against the average piston speed, \bar{U} .

$$U' = U / \bar{U}$$

The piston acceleration is normalized against the mean piston acceleration, \bar{U}^2 / R .

$$\ddot{Y}' = \ddot{Y} / (\bar{U}^2 / R)$$

3.2 Dimensionless Equations

Reynold's Equation

$$\frac{\partial}{\partial x'} (h'^3 \frac{\partial P'}{\partial x'}) - [3VT] \cdot U' \frac{\partial h'}{\partial x'} - \pi_2 \frac{\partial h'}{\partial t'} = 0 \quad (3.2-1)$$

This equation is normalized against $P_e \bar{h}^3 / W^2$.

Moment Balance

$$\begin{aligned} & - \pi_3 \frac{d^2 \alpha'}{dt'^2} + [R^2] (P_0' - P_1') \left(1 - \frac{\alpha'}{\alpha_0'}\right) - [S] \cdot \alpha' \\ & - 2 \int_0^1 (P' - P_0') (1 - x') dx' + 1 + \pi_6 hr' - [R/\Omega] \frac{\alpha'}{\alpha_0'} \ddot{Y}' \\ & - \pi_7 \left(1 - \frac{\alpha'}{\alpha_0'}\right) \int_0^1 h' \frac{\partial P'}{\partial x'} dx' + [R \cdot V] \cdot \left(1 - \frac{\alpha'}{\alpha_0'}\right) \int_0^1 U' \frac{dx'}{h'} = 0 \end{aligned} \quad (3.2-2)$$

This equation is normalized against the ring elastic force moment, $P_e W^2 / 2$.

Radial Force Balance

$$-\pi_{10} \frac{d^2 h_r'}{dt'^2} + \int_0^1 (P' - P_0') dx' - 1 - \pi_{11} \cdot h_r' = 0 \quad (3.2-3)$$

This equation is normalized against the pre-stressed ring force, $P_e W$.

Axial Force Balance

$$\begin{aligned} & -\pi_{12} \frac{d^2 h_a'}{dt'^2} + [12 R/V] \cdot \left(1 - \frac{\alpha'}{\alpha_0'}\right) (P_0' - P_1') \\ & + \pi_{14} \int_0^1 \frac{\partial P'}{\partial x'} dx' - 6U' \int_0^1 \frac{dx'}{h'} - [6/\Omega/V] \cdot \ddot{Y}' + \frac{6hF}{\eta \bar{U}W} = 0 \end{aligned} \quad (3.2-4)$$

This equation is normalized against the nominal film shear force, $\eta \bar{U}W / (6\bar{h})$.

3.3 Dimensionless Parameter List and Term Size

The non-dimensional parameter π 's in section 3.2 are listed below. In order to make a specific point concerning the terms in the non-dimensional equation, the case of a modified Citation engine is used. The physical data are in the input file DATA7. This engine is operating at 3000 RPM.

Name	Composition	Term size
$3V \cdot T$	$(6\bar{U}\bar{n}W)/(P_e\bar{h}^2)$	490
π_2	$(12\bar{U}\bar{n}W^2)/(P_e\bar{h}^2R)$	38
π_3	$(2\rho J\bar{U}^2\bar{\alpha})/(P_eR^2)$	3.7E-5
\mathcal{R}^2	$B^2/(4W^2)$	1.17
S	$(EBW)/(6P_eR_{cyl}^2)$	0.175
π_6	$(5EB^3\bar{h})/(3\pi^4 P_eR_{cyl}^4)$	0.0014
π_7	$(\bar{h}B)/(2W^2)$	0.0016
$\mathcal{R} \cdot V$	$(\bar{n}\bar{U}B)/(P_e\bar{h}W)$	0.216
\mathcal{R}/Ω	$(\rho\bar{U}^2 B^2)/(P_eWR)$	1.6
π_{10}	$(2\rho\bar{h}B\bar{U}^2)/(P_eR^2W)$	4E-5
π_{11}	$(5EB^3\bar{h})/(3\pi^4 P_eR_{cyl}^4)$	0.0014
π_{12}	$(6\rho B\bar{U}\bar{h}^2)/(\bar{n}R^2)$	4E-5
$12 \mathcal{R}/V$	$(3P_e\bar{h}B)/(\bar{n}\bar{U}W)$	54
π_{14}	$(3P_e\bar{h}^2)/(\bar{n}\bar{U}W)$	0.037
$6/\Omega/V$	$(6\rho\bar{U}\bar{h}B)/(\bar{n}R)$	36.5

where

$\mathcal{R} = B/(2W)$	Ring aspect ratio
$S = (EBW)/(6P_eR_{cyl}^2)$	Ring stiffness ratio
$T = W / \bar{h}$	Ring thickness number
$V = (2\bar{n}\bar{U})/(P_e\bar{h}) = (2\bar{n}(RPM)R)/(15P_e\bar{h})$	Ring pressure ratio
$\Omega = (P_eR)/(2\rho\bar{U}^2 B) = 225P_e/(2\rho(RPM)^2RB)$	Frequency

CHAPTER 4

Quasi-Static Models and Dynamic Simulation

4.1 Dynamic Simulation Evaluation

The classical method to generate the time history data of a state variable uses the Talor Series time expansion of the state variables such as film height, ring inclination angle, and ring axial position. The calculation proceeds in small time increments and calculate the time derivatives of the state variables. The derivatives are then inserted into the Talor's expansion to calculate the values of the state variables at the next time. This is one way to solve for the time history of the state variables.

However, this method has a limit: the size of the time increment. Levy and Kroll (1951) has shown that the optimum step size is approximately one-twentieth of the natural frequency, hence the smallest time step. Thus, this small time step limits the speed that calculation can proceed.

Let us take an example with a midium sized engine running at 520 RPM. Let the cylinder radius be 0.1 meter. Let the bronze ring density be 8800 Kg/m^3 density and ring dimensions be 14 by 9 mm. The natural frequency is associated with ω , where

$$\omega^2 = C_{tw} / \rho J$$

where J is the polar moment of inertia of the ring.

For the given, ω is about $1.9E4$ radians per second. Therefore, the natural period is $3.2E-4$ second; the optimum time step is $1.6E-5$ second. At this pace, it would take 14400 steps to calculate a four stroke cycle cycle. With the available PDP 11/60 computer, it would take ten hours!

The way to circumvent this long calculation is to make another approximation: Quasi-Static state of operation. The ring state variables changes slowly for most of the cycle, except near the turning points where the accelerations and the velocities are high. For the most part, the effect of the time derivatives are relatively small; therefore, we neglect them.

Since the time derivatives are no longer considered, we may consider each point of operation (in time) separately. As a result, the behavior of the ring may be examined through the discrete history of the state variables h_r and α .

Furthermore, the number of the dynamic equations that needs to be evaluated simultaneously may be reduced from three to two. Since the ring stays on the wall, and the axial force equation is decoupled from the moment balance and the radial force balance.

4.2 Analytical Approximation

The bulk of the computation work are done on the hydrodynamic force. In the most general case, for an arbitrary ring contour, it is necessary to use finite difference method to approximate the pressure in the oil film under the ring. This is very laborous, even if it is done on a digital computer. The rational, therefore, is to seek a profile that can generate the forces similar to those of the simulated ring. We have two such profiles: Effective Slope (ES), and the Composite Secant (CS). They are both described by Cameron.

4.3 Simplifications

4.3.1 Simplified Equations

From equation 3.2-1, we note that the first term, $[3VT]$, is generally ten times larger than the second term, π_{12} . (However, for U' smaller than 0.1, the first term is then comparable in size with the second.) This means that we can generally neglect the second term except where U' is small. Then 3.2-1 becomes

$$\frac{\partial}{\partial x'} (h'^3 \frac{\partial P'}{\partial x'}) = [3V \cdot T] \cdot U' \frac{\partial h'}{\partial x'} \quad (4.3-1)$$

For equation 3.2-2, the moment equation, π_3 , π_6 , and π_7 vanishes in comparison with other terms. So eq. 3.2-2 simplifies to

$$[R^2] \cdot \Delta P' (1 - \alpha' / \alpha_0') - [S] \cdot \alpha' - 2 \int_0^1 (P' - P_0') (1 - x') dx'$$

$$+ 1 + [\mathcal{R}/\Omega] \cdot (\alpha'/\alpha_0') + [\mathcal{R} \cdot V] \cdot (1 - \alpha'/\alpha_0') U' \int_0^1 \frac{dx'}{h'} = 0 \quad (4.3-2)$$

For equation 3.2-3, the radial force balance, π_{10} and π_{11} terms are neglected. So

$$\int_0^1 (P' - P_0') dx' - 1 = 0 \quad (4.3-3)$$

(This means that the difference of lift and back gas force must be equal to the elastic pressure force.)

For equation 3.2-4, the axial force balance, π_{12} and π_{14} are smaller than the others, so

$$[12\mathcal{R}/V] \cdot \Delta P_1' (1 - \alpha'/\alpha_0') - [6/\Omega/V] \cdot \bar{Y}' + \frac{6\bar{h}F}{\eta\bar{U}W} = 0 \quad (4.3-4)$$

This means that the difference of pressure force and the d'Alembert force is supplied by the ring groove lands.

4.3.2 Simplified Dimensionless Parameter List

Deleting the smaller terms, and assuming \ddot{Y}' and U' are large, in the order of unity, we have the following left.

Name	Composition	Size
3VT	$(6\bar{U}\eta W)/(P_e \bar{h}^2)$	490
\mathcal{R}^2	$B^2/(4W^2)$	1.17
S	$(EBW)/(6P_e R_{cyl}^2)$	0.175
$\mathcal{R} \cdot V$	$(\eta \bar{U} B)/(P_e \bar{h} W)$	0.216
\mathcal{R}/Ω	$(\rho \bar{U}^2 B^2)/(P_e W R)$	1.59
12 R/V	$(3P_e \bar{h} B)/(\eta \bar{U} W)$	54
$6/(\Omega \cdot V)$	$(6\rho \bar{U} h B)/(\eta R)$	36

where

$\mathcal{R} = B/(2W)$	Ring aspect ratio
$S = (EBW)/(6P_e R_{cyl}^2)$	Ring stiffness number
$T = W / \bar{h}$	Ring thickness number
$V = (2\eta \bar{U})/(P_e \bar{h}) = 2\eta R(\text{RPM})/(15P_e \bar{h})$	Ring pressure ratio
$\Omega = (P_e R)/(2\rho \bar{U}^2 B) = 225P_e/(2\rho R B(\text{RPM})^2)$	Frequency

CHAPTER 5

Effective Slope Model

5.1 Geometry and Forces

The rationale is simple: replace the curved surface by a simple flat surface. Since the lift generated by any two surfaces that have the same inlet and outlet dimensions differs at most ten percent, this may be a good approximation. Thus, we define a fixed plane in the ring as presented:

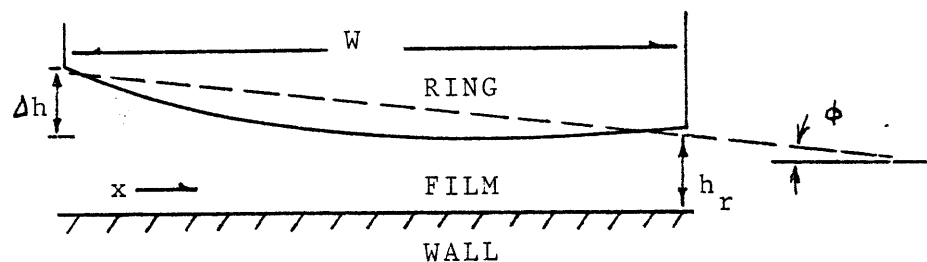


Fig. 5.1-1 Effective slope film

The pressure field is contributed by two pressure field elements: pressure drop across the ring, and the film drag. Conveniently, these two fields may be superpositioned to form the physical pressure field. Therefore, we shall first treat the pressure field from film drag.

Substituting $h_r + \alpha x$ for h in Reynold's equation, and integrate

once for the width of the ring, Cameron¹ has shown that the pressure distribution is

$$P = \frac{6U\eta W}{K} \frac{1}{h_r} \left[-\frac{1}{h} - \frac{h_r h_1}{h^2 (h_1 + h_r)} - \frac{1}{(h_1 + h_r)} \right] \quad (5.1-1)$$

$$\text{where } K = \phi W / h_r \quad (5.1-2)$$

Integrate again to obtain the load (per unit ring length)

$$\text{Lift} = \frac{6U\eta W^2}{h_r^2} \frac{1}{K^2} \left[\ln\left(\frac{h_1}{h_r}\right) - \frac{2(h_1 - h_r)}{(h_1 + h_r)} \right] \quad (5.1-3)$$

replace by K,

$$\text{Lift} = \frac{6U\eta}{\phi^2} \left[\ln(K+1) - \frac{2K}{(K+2)} \right] \quad (5.1-4)$$

Similarly, we may find the center of pressure from the trailing edge to be

$$\bar{x}^* = \frac{K+1}{K} \left[\frac{K-2}{2} + \frac{\ln(K+1)}{K} \right] = \frac{x^*}{W} \quad (5.1-5)$$

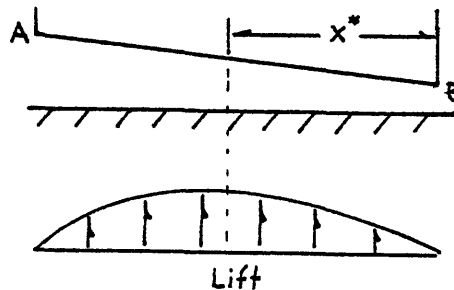


Fig.5.1-1 Center of pressure of oil moment

For the pressure field by the pressure drop, the lift is

¹ Cameron, Alastair, Basic Lubrication Theory, Ch.5, pp.48-55.

$$\text{Lift} = \Delta P_1 W (K+1) / (K+2) \quad (5.1-6)$$

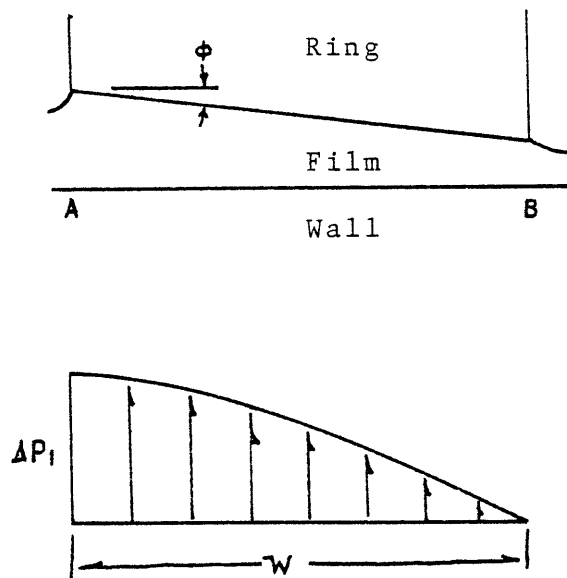


Fig.5.1-2 Pressure drop across the ring by ΔP_1

The moment about point B is

$$M_B = \frac{\Delta P_1 W}{K^2} \left[\frac{(K+1)^2}{2} - \frac{(K+1)^2}{K(K+2)} \ln(K+1) - \frac{K(K+1)}{(K+2)} \right] \quad (5.1-7)$$

When calculating using the effective slope model, we substitute the lift moments and the lift forces into the corresponding terms of the governing force equations.

5.2 Computational organization

For practical purposes, there are four modes that the ring is in. See Figure 5.2-1. We define $F1(\phi, h_r)$ as the residue of the force balance and define $F2(\phi, h_r)$ as the moment balance residue. When the residues are both zero, the variables ϕ and h are the values of the state variables.

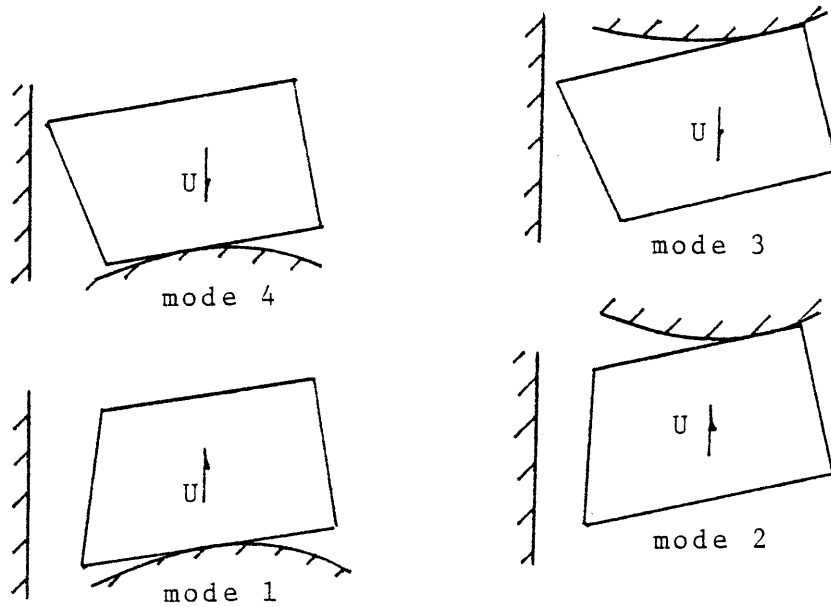


Fig. 5.2-1 Ring modes in ES model

Fortunately, for the linear profile, there is analytical solution. Even more so, is that when the oil pressure lift term is inserted into the radial force balance equation, the equation may be simplified further. For a typical ring mode, for example, ring at bottom and travelling downward, the equation is

$$F_1 = -P_e W - \Delta P_1 W + \Delta P_1 W \frac{(K+1)}{(K+2)} + \frac{6U\bar{u}W^2}{h^2 h'^2} \frac{1}{K^2} \left[\ln(K+1) - \frac{2K}{(K+2)} \right] = 0 \quad (5.2-1)$$

It is now more profitable to change F_1 to a new set of state variables (ϕ', K) , and non-dimensionalized against $P_e W$,

$$\text{where } K = (\phi W / \bar{h})(\phi' / h') \quad (5.2-4)$$

then Equation (5.2-1) becomes

$$-1 - \frac{\Delta P_1}{P_e} \frac{K+1}{K+2} + \frac{6\bar{u}\eta}{P_e \bar{W} \alpha^2} \frac{1}{\phi'^2} \left[\ln(K+1) - \frac{2K}{(K+2)} \right] = 0 \quad (5.2-3)$$

Solve for ϕ' , and get

$$\phi' = \left[\frac{6U\eta}{W\alpha^2 P_e} \frac{[\ln(K+1) - 2K/(K+2)]}{[1+(\Delta P_1/P_e)(K+1)/(K+2)]} \right] = \frac{\phi}{\alpha} \quad (5.2-4)$$

Given ϕ' and K , we may solve for the residue of F2, by the following

$$\begin{aligned} F2 = & \Delta P_1 \frac{B^2}{8} [1 - (\phi' - \alpha_0')/\alpha_0'] - P_e \frac{W^2}{2} - \Delta P_1 \frac{W^2}{2} \\ & - \left(\frac{EBW^3 \bar{\alpha}}{12 R_{cyl}^2} + \frac{\rho B^2 \bar{\alpha} Y}{2 \alpha_m} \right) (\phi' - \alpha_0') \\ & + \frac{6U\eta W}{\alpha \phi'^2} [\ln(K+1) - \frac{2K}{(K+2)}] \left[\frac{K(K+6) - (4K+6)\ln(K+1)}{2K((K+2)\ln(K+1) - 2K)} \right] \\ & + \Delta P_1 W^2 \left[\frac{(K+1)^2}{2K^2} - \frac{(K+1)^2}{K^3(K+2)} \ln(K+1) - \frac{(K+1)}{K(K+2)} \right] \\ & - \frac{B}{2} [1 - (\phi' - \alpha_0')/\alpha_0'] \left[\frac{\eta U}{\alpha \phi'} \ln(K+1) + \Delta P_1 \frac{\phi'(K+1)}{\alpha W K(K+2)} \right] = 0 \end{aligned} \quad (5.2-5)$$

We may also represent F2 in non-dimensional form:

$$\begin{aligned} F2' = & \frac{\Delta P_1 B^2}{4P_e W^2} [1 - (\alpha' - \alpha_0')/\alpha_0'] - 1 - \frac{\Delta P_1}{P_e} \\ & - \left(\frac{EBW \bar{\alpha}}{6P_e R_{cyl}^2} + \frac{\rho B^2 \bar{\alpha} Y}{P_e W \alpha_m} \right) (\phi' - \alpha_0') \\ & + \frac{12 U \eta}{P_e \alpha^2 W \phi'^2} [\ln(K+1) - \frac{2K}{(K+2)}] \left[\frac{K(K+6) - (4K+6)\ln(K+1)}{2K((K+2)\ln(K+1) - 2K)} \right] \\ & + \frac{2\Delta P_1}{P_e} \left[\frac{(K+1)^2}{2K^2} - \frac{(K+1)^2}{K^3(K+2)} \ln(K+1) - \frac{(K+1)}{K(K+2)} \right] \end{aligned}$$

$$- [1 - (\phi' - \alpha_0') / \alpha_0'] \left[\frac{B\eta U}{P_e W^2 \alpha \phi'} \ln(K+1) + \frac{2\Delta P_1 \bar{\alpha} \phi'(K+1)}{P_e W^2 K(K+2)} \right] = 0 \quad (5.2-6)$$

Thus, by using the effective slope, the two simultaneous equations F1 and F2 are reduced to one equation - F2'(K).

The root of the equation F2'=0 is the solution to the original state variables h_r' and ϕ' ; therefore, it is necessary to solve for K.

The numerical method that is most likely to yield the solution is the bisection method. This scheme operates on the principle that if the function F2'(K) is continuous over the interval $[K_a, K_b]$, and the residues at K_a and K_b are of opposite sign, then there must be at least one solution in the interval. This program ESMOD uses a modified bisection method based on the algorithm from a Texas Instruments Solid State Software Program ML-08. For details, see attached flow chart in Appendix A2.

Upon solving K, we insert K into Equation (5.2-4) to get ϕ' . Then the dimensionless ring tilt angle is $\alpha' = \phi' - \alpha_0'$. From ϕ' and K we find h_r' . These yield the friction:

$$F_{\mu}' = \frac{-6\bar{h}\bar{U}}{\alpha\bar{U}\bar{W}\phi'} \ln(K+1) - \frac{6\bar{h}\Delta P_1 \bar{\alpha} \phi'(K+1)}{\eta\bar{U} K(K+2)} \quad (5.2-7)$$

$$F_{\mu} = F_{\mu}' \left(\frac{\bar{U}\eta\bar{W}}{6\bar{h}} \right) \quad (5.2-8)$$

where F_{μ}' is the dimensionless friction, and F_{μ} is the physical friction.

5.3 Input/Output

The input variables that this program need is listed in the program listing in Appendix A3. It is fed to the program in a data file, DATA4.

The first block of this data file contains the physical, operational, and geometrical information. The physical data include crank rod length, crank radius, ring elastic pressure, oil viscosity and density, ring density, and modulus of elasticity. The operational data include speed and compression ratio. The geometrical information include the maximum ring tilt angle and the ring dimensions. In addition, limits for iteration are included.

The data file also supply the program data to run a simplified version of pressure routine to calculate the cylinder pressure under combustion.

The final block of data contains the crank angles that the state variables are to be evaluated.

The output is written into a data file also, DATA5, and it is monitored on the CRT screen simultaneously.

The following is in the output file:

1. Crank angle
2. Pressure differential across the ring in atm
3. Non-dimensional reference film height
4. Non-dimensional effective slope
5. Non-dimensional ring tilt angle
6. Non-dimensional friction
7. Piston position
8. Piston velocity
9. Piston acceleration
10. K
11. Mode of the ring

At the end of the file, the I_{mep} and the F_{mep} are displayed, as well as other physical data. For details, refer to Appendix A4.

CHAPTER 6

Composite Secant

The deficiency of the effective slope concept is that it does not represent the ring contour very well. Furthermore, it is difficult to choose an effective slope that best represents an arbitrary contour. Thus, it is very much limited to as an intellectual exercise, even though it has shed much insight into the oil film thickness, ring inclination, and friction.

The composite secant², however, fills some of the deficiencies. Three points can define the curved surface which formed the two secant curves joined back to back at their origins. This shape approximates the real ring shape more closely, and its associated oil pressure moment distribution also resembles the actual moment distribution. Furthermore, this scheme allows changes in the physical characteristics of the ring surface, such as ring profile heights, and the location of the profile peak.

6.1 Geometry and Pressure Field

The physics of the model is sketched in figure 6.1-1.

²Cameron, Alastair, Basic Lubrication Theory, Ch.4

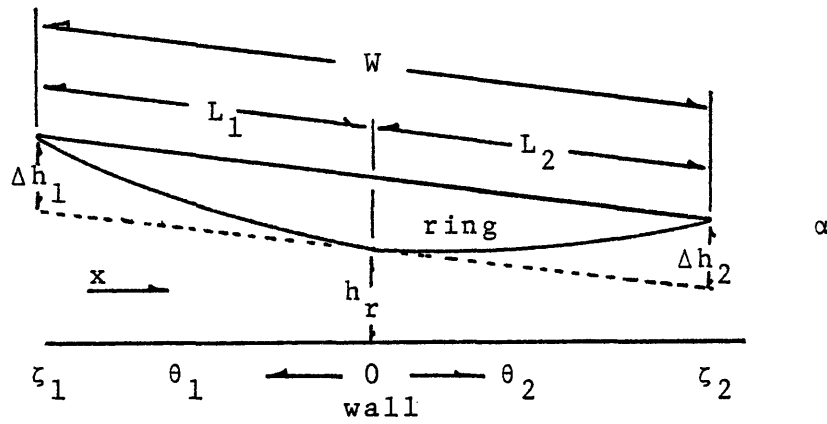


Fig. 6.1-1 Composit Secant Film

Cameron used the secant film because it was relatively easy to integrate. The author chose to use this shape, also because that the slope of the secant at the origin is zero. Thus the two secants may form a smooth curve.

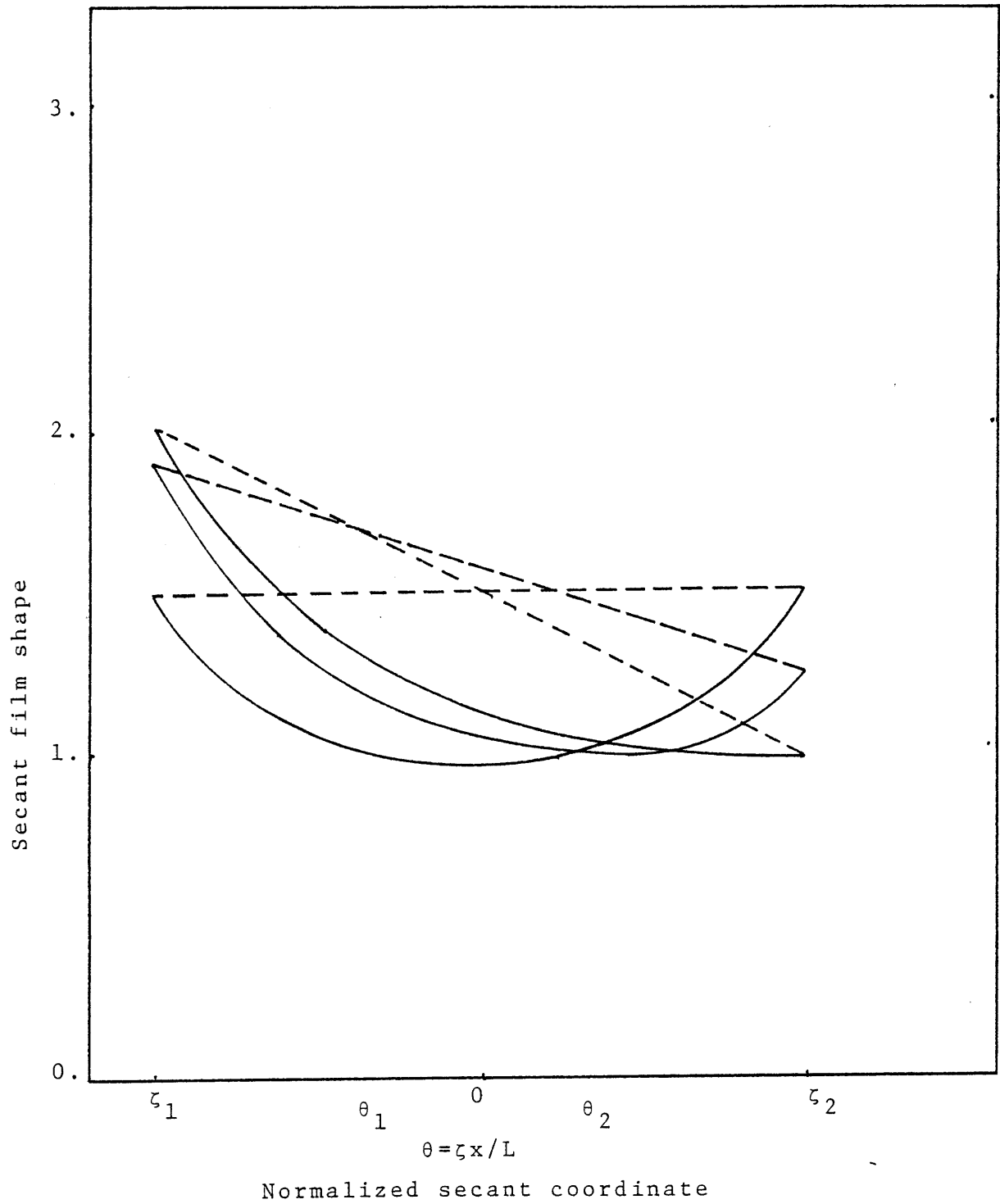


Fig. 6.1-2 Change of Tilt Angle on CS Film Shape

The secants for the convergent-divergent channel between the ring and the cylinder changes shape when there are changes in the reference film height, h_r , or inclination angle, α . Figure 6.1-2 illustrates this.

The Coordinates under the Ring is normalized with respect to the ring width, W . The position coordinate x is transferred to coordinate ζ . The following represents the transformation:

$$\text{Sec } \zeta_1 = (\Delta h_1 + \alpha L_1) / h_r + 1 ; \quad \theta_1 = \zeta_1 (x_1 / L_1) \quad (6.1-1)$$

$$\text{Sec } \zeta_2 = (\Delta h_2 - \alpha L_2) / h_r + 1 ; \quad \theta_2 = \zeta_2 (x_2 / L_2) \quad (6.1-2)$$

To find the pressure field, again, we integrate, substituting $h_r \text{Sec } \zeta_1$ for h . The pressure function for a secant film in terms of a normalized coordinate ζ is then

$$P = \frac{-6U\eta L}{\zeta h_r} \frac{1}{2} [-(\theta + \text{Sin } \theta \text{Cos } \theta) - \frac{\text{Sec } \bar{\theta}}{3} \text{Sin } \theta (2 + \text{Cos } \theta) + C] \quad (6.1-3)$$

There is one equation for each one of the secant curves.

6.2 Boundary Conditions

Since there are two secant curves, then there are two fields that need to be matched by boundary conditions. Let the left side be subscripted (1) and the right side be (2).

There are four boundary conditions.

1. At $\theta_1 = \zeta_1$. $P = \Delta P_1 = P_0 - P_1$ Combustion pres.

2. At $\theta_2 = \zeta_2$, $P=0$ Crank case pres.
3. At $\theta_1 = \zeta_2 = 0$ Pressure matches
4. At $\theta_1 = \zeta_2 = 0$ Pres. gradient matches

$$\frac{dP_1}{dx_1} \Big|_{x_1=0} = - \frac{dP_2}{dx_2} \Big|_{x_2=0} \quad (6.2-1)$$

The sign is negative because the two coordinate systems are in the opposite directions.

From condition 3, the following can be shown:

$$-L_1 C_1 / \zeta_1 = L_2 C_2 / \zeta_2 \quad (6.2-2)$$

When C_1 and C_2 are constants in the P equation.

Applying condition 1, we have constant C_1 from film 1

$$C_1 = \frac{-\Delta P_1 \zeta_1 h_r}{6U\eta L_1} - \frac{1}{2} [\zeta_1 + \sin \zeta_1 \cos \zeta_1] + \frac{\sec \theta_1}{3} \sin \zeta_1 (2 + \cos \zeta_1) \quad (6.2-3)$$

Applying condition 2, we have constant C_2 from film 2

$$C_2 = - \frac{1}{2} [\zeta_2 + \sin \zeta_2 \cos \zeta_2] + \frac{\sec \theta_2}{3} \sin \zeta_2 (2 + \cos \zeta_2) \quad (6.2-4)$$

Applying condition 4, we have

$$\bar{\theta}_1 = \bar{\theta}_2 \quad (\text{surprise!})$$

(Note: $\frac{dP_1}{dx_1}$ and $\frac{dP_2}{dx_2}$ are evaluated, not $\frac{dP_1}{d\theta_1}$ and $\frac{dP_2}{d\theta_2}$!) and sub-

stituting C_1 and C_2 into eq. 6.1-5, and equate, we obtain

$$\sec \theta = \frac{\frac{\Delta P_1 h_r^2}{6U\eta} + \frac{W}{2} + \frac{L_1 \sin \zeta_1 \cos \zeta_1}{2\zeta_1} + \frac{L_2 \sin \zeta_2 \cos \zeta_2}{2\zeta_2}}{\frac{\sin \zeta_1 (\cos \zeta_1 + 2)L_1}{3\zeta_1} + \frac{\sin \zeta_2 (\cos \zeta_2 + 2)L_2}{3\zeta_2}} \quad (6.2-5)$$

6.3 Oil Forces and Moments

Integrating each of the pressure fields across its own width, and combining them,

$$\begin{aligned} \text{Lift} = & \frac{6U\eta}{h_r^2} \left[\left[\frac{L_2}{\zeta_2} \right]^2 \left[\frac{\zeta_2^2}{4} + \frac{\sin^2 \zeta_2}{4} - \frac{\sec \bar{\theta}}{3} \left(\frac{\sin \zeta_2}{2} \right. \right. \right. \\ & \left. \left. \left. - 2\cos \zeta_2 + 2 \right) + C_2 \zeta_2 \right] - \left[\frac{L_1}{\zeta_1} \right] \left[\frac{\zeta_1^2}{4} + \frac{\sin^2 \zeta_1}{4} \right. \right. \\ & \left. \left. - \frac{\sec \bar{\theta}}{3} \left(\frac{\sin \zeta_1}{2} - 2\cos \zeta_1 + 2 \right) + C_1 \zeta_1 \right] \right] \quad (6.3-1) \end{aligned}$$

The moment about the joining point is

$$\begin{aligned} M = & \frac{-6U\eta}{h_r^2} \left[\left[\frac{L_1}{\zeta_1} \right]^3 \left[\frac{\zeta_1^3}{6} + \frac{\sin 2\zeta_1}{16} - \frac{\zeta_1}{8} \cos 2\zeta_1 + \right. \right. \\ & \left. \left. \frac{2\sec \bar{\theta}}{3} \left(\zeta_1 \cos \zeta_1 - \sin \zeta_1 - \frac{\sin 2\zeta_1}{16} + \frac{\zeta_1 \cos 2\zeta_1}{8} \right) \right. \right. \\ & \left. \left. C_1 \frac{\zeta_1^2}{2} \right] + \left[\frac{L_2}{\zeta_2} \right]^3 \left[\frac{\zeta_2^3}{6} + \frac{\sin 2\zeta_2}{16} - \frac{\zeta_2}{8} \cos 2\zeta_2 - \frac{2\sec \bar{\theta}}{3} \right. \right. \\ & \left. \left. \left(\zeta_2 \cos \zeta_2 - \sin \zeta_2 - \frac{\sin 2\zeta_2}{16} + \frac{2\cos 2\zeta_2}{8} \right) + C_2 \frac{\zeta_2^2}{2} \right] \right] \quad (6.3-2) \end{aligned}$$

The total friction is then, from Eq. (6.3-3)

$$\begin{aligned} F_u = & \frac{-L_1 U \eta}{h_r \zeta_1} \sin \zeta_1 - \frac{L_1 U \eta}{h_r \zeta_2} \sin \zeta_2 \\ & - \frac{3U\eta L_1}{h_r \zeta_1} \left(\sin \zeta_1 - \zeta_1 \frac{\sec \bar{\theta}}{2} - \frac{\sec \bar{\theta}}{4} \sin 2\zeta_1 \right) \end{aligned}$$

$$+ \frac{3U\eta L_2}{\zeta_2 h_r} (\sin \zeta_2 - \zeta_2 \frac{\sec \bar{\theta}}{2} - \frac{\sec \bar{\theta}}{4} \sin 2\zeta_2) \quad (6.3-3)$$

6.4 Total Forces and Moments

Substituting the expression of equation 6.3-1 into equation 2.4-3 for the lift force and normalize with respect to $P_e W$, we have (for ring at bottomland) the dimensionless radial force equation.

$$F1' = -1 - \frac{\Delta P_1}{P_e} + \frac{6U\eta L_1^2}{P_e W h^2} \frac{1}{h_r'} \frac{L_2}{L_1} \left[\left(\frac{L_2}{L_1} \right)^2 \right. \\ \left. - \frac{1}{L_2^2} \left[\frac{\zeta_1^2}{4} + \frac{\sin^2 \zeta_2}{4} - \frac{\sec \bar{\theta} \sin \zeta_2}{3} \left(\frac{\sin \zeta_2}{2} - 2\cos \zeta_2 + 2 \right) + C_2 \zeta_2 \right] \right. \\ \left. - \frac{1}{\zeta_1^2} \left[\frac{1}{4} + \frac{\sin^2 \zeta_1}{4} - \frac{\sec \bar{\theta} \sin^2 \zeta_1}{3} \left(\frac{\sin^2 \zeta_1}{2} - 2\cos \zeta_1 + 2 \right) + C_1 \zeta_1 \right] \right] \quad (6.4-1)$$

Substituting equation 6.3-3 for drag and 6.3-2 for the oil moment in equation 2.4-2 and normalize with $P_e W^2/2$, we have the dimensionless moment equation.

$$F2' = \left[\frac{\Delta P_1 B^2}{4P_e W^2} \right] [1 - \alpha' / \alpha_0']^2 + \frac{\Delta P_1}{P_e} + 1 - \frac{EBW\bar{\alpha}}{6P_e R_{cyl}^2} \alpha' \\ - \frac{\rho B^2 Y \bar{\alpha}}{P_e W \alpha_m} + \left[\frac{L_1 U \eta B}{P_e W^2 h} \right] \frac{1}{h_r'} \left[\frac{\sin \zeta_1}{\zeta_1} + \left(\frac{L_2}{L_1} \right) \frac{\sin \zeta_2}{\zeta_2} + \frac{3}{\zeta_1} \right. \\ \left. (\sin \zeta_1 - \zeta_1 \frac{\sec \bar{\theta}}{2} - \frac{\sec \bar{\theta}}{4} \sin 2\zeta_1) - \frac{3}{\zeta_2 L_1} \left(\frac{L_2}{L_1} \right)^3 (\sin \zeta_2 \right. \\ \left. - \zeta_2 \frac{\sec \bar{\theta}}{2} - \frac{\sec \bar{\theta}}{4} \sin 2\zeta_2) \right] - \left[\frac{12U\eta L_1^2 L_2}{P_e W^2 h^2} \right] \frac{1}{h_r'^2} \\ \left[\frac{1}{\zeta_2^2} \left(\frac{L_2}{L_1} \right)^2 \left[\frac{\zeta_2^2}{4} + \frac{\sin^2 \zeta_2}{4} - \frac{\sec \bar{\theta} \sin^2 \zeta_2}{3} \left(\frac{\sin^2 \zeta_2}{2} - 2\cos \zeta_2 + 2 \right) \right] \right]$$

$$\begin{aligned}
& C_2 \zeta_2] - \frac{1}{\zeta_1^2} \left[\frac{\zeta_1^2}{4} + \frac{\sin^2 \zeta_1}{4} - \frac{\sec \bar{\theta}}{3} \left(\frac{\sin^2 \zeta_1}{2} - 2 \cos \zeta_1 \right. \right. \\
& \left. \left. + 2 \right) + C_1 \zeta_1 \right] - \left[\frac{12 \eta U L_1^3}{\rho_e W^2 h} \right] \frac{1}{h_r'^2} \left[\frac{1}{\zeta_1^3} \left[\frac{\zeta_1^3}{6} + \frac{\sin 2\zeta_1}{16} \right. \right. \\
& \left. \left. - \frac{\zeta_2}{8} \cos 2\zeta_1 + \frac{2 \sec \bar{\theta}}{3} (\zeta_1 \cos \zeta_1 - \sin \zeta_1) - \frac{\sin 2\zeta_1}{16} + \frac{\zeta_1 \cos 2\zeta_1}{8} \right. \right. \\
& \left. \left. + C_1 \frac{\zeta_1^2}{2} \right] + \frac{1}{\zeta_2^3} \left[\frac{L_2}{L_1} \right]^3 \left[\frac{\zeta_2^3}{6} + \frac{\sin 2\zeta_1}{16} - \frac{\zeta_2}{8} \cos 2\zeta_2 + \frac{2 \sec \bar{\theta}}{3} \right. \\
& \left. \left. (\zeta_2 \cos \zeta_2 - \sin \zeta_2 - \frac{\sin 2\zeta_2}{16} + \frac{\zeta_2 \cos 2\zeta_2}{8}) + C_2 \frac{\zeta_2^2}{2} \right] \right] \quad (6.4-2)
\end{aligned}$$

Substituting eq. 6.3-3 into the drag term of eq. 2.4-4 and normalize with respect to $\eta \bar{U} W / (6 \bar{h})$, we have the dimensionless axial force eq.

$$\begin{aligned}
F_3' &= \frac{-\Delta P_1 B \bar{h}}{2 \bar{U} \eta W} [1 - \alpha' - \alpha_0'] - \frac{L_1 \sin \zeta_1}{W \zeta_1 h_r'} - \frac{L_2 \sin \zeta_2}{W 2 h_r'} \\
&+ \frac{-3 U L_1}{\bar{U} W} \frac{1}{\zeta_1 h_r'} (\sin \zeta_1 - \zeta_1 \frac{\sec \bar{\theta}}{2} - \frac{\sec \bar{\theta}}{4} \sin 2\zeta_1) \\
&+ \frac{3 U L_2}{\bar{U} W} \frac{1}{\zeta_2 h_r'} (\sin \zeta_2 - \zeta_2 \frac{\sec \bar{\theta}}{2} - \frac{\sec \bar{\theta}}{4} \sin 2\zeta_2) \\
&- \frac{\rho B Y \bar{h}}{\bar{U} \eta} + F' = 0 \quad (6.4-3)
\end{aligned}$$

For ring at topland, see Appendix B1 for equations.

6.5 Computational Organization

The beginning of the composite secant model program is very much the same as the ES model program. However, due to the transcendental nature of the equations, an extra step is taken.

Unlike the ES model, neither the radial force equation (F1) nor the moment balance equation (F2) can be simplified further. So it is necessary to solve two non-linear equations with two variables, as it is.

Adapting the same procedure as the ES model, this computation program, COMSEC, uses the same bisection method as the ES program to solve for the roots to the equations. However, because there are now two equations, there must be two iteration loops, with one nested in the other.

In this scheme, the program assumes a ring inclination angle, α_a . Substituting α_a into F1, the force equation, the subroutine BISHR solves for the h_{ra} where $F1=0$ is satisfied. The program then assumes another α_b , and solves for h_{rb} with BISHR. Substituting h_{ra} and α_a into F2, the moment equation, subroutine MOMENT, yields the residue of $F2(h_{ra}, \alpha_a)$. Similarly, we obtain $F2(h_{rb}, \alpha_b)$. If the residues are of opposite sign, then there is solution between α_a and α_b . Subroutine BISALP solves for the α where $F2=0$.

The penalty brought on by the extra loop is that the number of calculations increases by a factor of n square, where n is the number of iterations in each loop. For the ES model, only $2n$ calculations are needed.

For each crank angle specified, the program will solve for the values of the state variable α and h_r and the friction. The algorithm is in Appendix B2.

6.6 Input/Output

The physical properties that this program requires are:

- connecting rod length
- crank radius
- ring axial width
- ring radial width
- piston bore diameter
- oil density
- oil viscosity
- ring density
- ring modulus of elasticity
- ring elastic pressure
- ring surface profile heights
- ring surface crest position

The operating conditions that the program needs are

- RPM
- compression ratio

The parameters that needed for numerical output are

epsilon.....convergence criterion for N-D height,
 usually 0.001
 epsilon.....convergence criterion for N-D angle,
 usually 0.001
 h_{ra}lower dimensionless film thickness,
 usually 0.01
 h_{rb}upper dimensionless film thickness,
 usually 20.1
 α_alower dimensionless tilt angle limit
 usually $-\alpha_0'$
 α_bupper dimensionless tilt angle limit
 usually $+\alpha_0'$

The output is similar to the output of ES model and is listed in tabular form:

1. Crank angle
2. Pressure difference across the ring in atm
3. Dimensionless film reference height
4. Dimensionless ring tilt angle
5. Dimensionless friction
6. Piston position
7. Piston velocity
8. Piston acceleration
9. Ring mode

In addition, F_{mep} and I_{mep} and other physical data are printed in the end of the list. The coefficient of friction is shown here. The nine parameters are arranged in a table suitable for plotting in the data file, DATA8.

CHAPTER 7

Results and Discussions

7.1 Computational Results

From the model of piston ring hydrodynamic lubrication, there are five primary similarity parameters. These are identified in section 3.3 and 4.3.2. The parameters S , R , and T are the geometric parameters that describe the ring and its physical parameters such as density and modulus of elasticity. Others, like V and Ω , are engine parameters that characterize the lubrication and piston kinematics. In addition, the frictional loss is characterized by the averaged coefficient of friction, C_f , the ratio of F_{mep} and the ring elastic pressure P_e .

The above five primary parameters were varied to determine the individual effect on the coefficient of friction. The parameters were varied about the following standard case where

$$R = 1.08$$

$$S = 1243$$

$$T = 1000$$

$$V = .358$$

$$\Omega = .701$$

The results are tabulated in table 7.1-1, and are plotted in Fig. 7.1-1 to 7.1-5.

7.2 Discussions

The effect of the aspect ratio (\mathcal{R}) on the coefficient of friction is approximately, from Fig. 7.1-1:

$$C_{\mu} = 0.0464 \left[\frac{\mathcal{R}}{1.08} (0.167 + 0.277 \log(\mathcal{R}/1.08)) \right]$$

Qualitatively, C_{μ} did not change much for low R in the range 0.3 to 1.0. The compression rings were often in this region. At higher R (near 4), C_{μ} increased much more quickly. The oil control rings were in this region. The higher friction from the oil control ring confirmed by Furuham, Takiguchi, and Tonizawa³, is apparently due to its higher elastic pressure.

The effect of ring stiffness number (S) on C_{μ} is approximately, from Fig. 7.1-2,

$$C_{\mu} = 0.0448 \left[\frac{S}{621} (0.052 + 0.087 \log(S/621)) \right]$$

The flatness of the C_{μ} curve means that using a stiffer or softer ring has little potential for altering the friction. This was not reported in any of the previous literatures.

³Furuham, Takiguchi, and Tonizawa, 'Effect of Piston and Piston Ring Design on the Piston Friction Forces in Diesel Engines,' SAE paper no. 810977. p.63-

Fixed Parameters				Physical Parameters		
	AR	C_u	Fmep(Psi)	B(m)	E(Pa)	ρ (Kg/m ³)
S=1243	0.271	.0424	.623	1.07E-3	8.2E11	3.16E4
T=1000	0.542	.0436	.641	2.15E-3	4.1E11	1.58E4
V=.357	1.08	.0464	.682	4.29E-3	2.1E11	7.90E3
Ω =.690	2.17	.0535	.786	8.59E-3	1.0E11	3.95E3
	4.33	.0660	.970	17.2E-3	5.1E11	1.98E3
	S	C_u	Fmep(Psi)	E(Pa)		
AR=1.08	124.	.0430	.632	2.05E10		
T=1000	248.	.0436	.641	0.41E11		
V=.357	621.	.0448	.658	1.02E11		
Ω =.690	1243	.0464	.682	2.05E11		
	2485	.0487	.716	4.10E11		
	T	C_u	Fmep(Psi)	\bar{h}	η (Pa-s)	
AR=1.08	250	.0826	1.21	7.92E-6	0.0134	
S=1243	500	.0610	.896	3.96E-6	0.00672	
V=.357	1000	.0464	.682	1.98E-6	0.00336	
Ω =.690						
	V	C_u	Fmep(Psi)	η (Pa-s)		
AR=1.08	0.178	.0284	.417	1.68E-3		
S=1243	0.356	.0464	.682	3.36E-3		
T=1000	0.725	.0773	1.14	6.72E-3		
Ω =.690	1.427	.132	1.94	13.4E-3		
	2.854	.232	3.42	26.9E-3		
	Ω	C_u	Fmep(Psi)	ρ (Kg/m ³)		
AR=1.08	.345	.0470	.691	15.8E3		
S=1243	.701	.0464	.682	7.90E3		
T=1000	1.40	.0461	.678	3.95E3		
V=.357	2.10	.0459	.675	2.63E3		
	2.80	.0458	.673	1.98E3		

Table 7.1-1 Variations of the coefficient of friction with respect to variations in the primary dimensionless parameters.

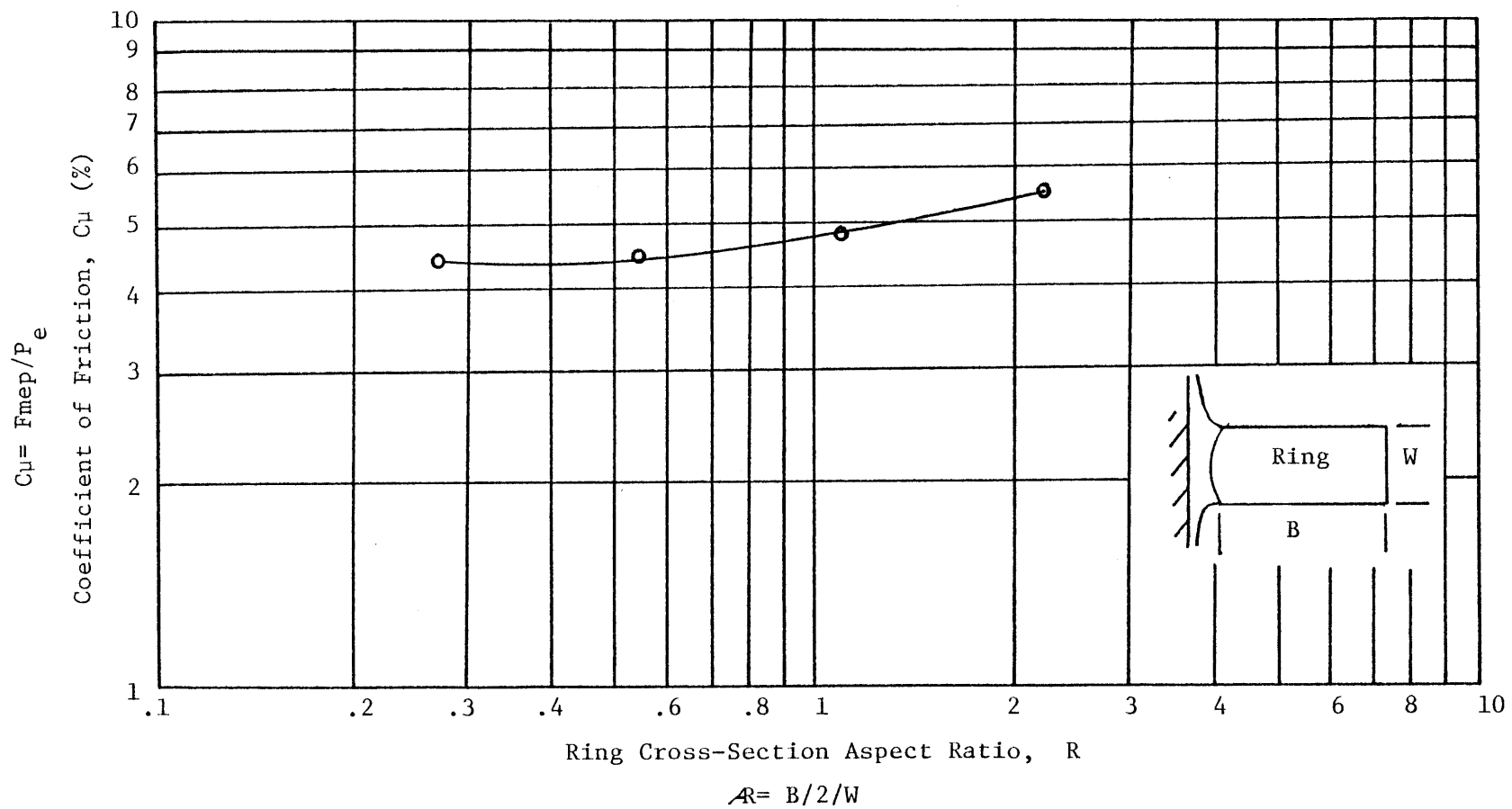


Figure 7.1-1 Coefficient of friction versus ring aspect ratio

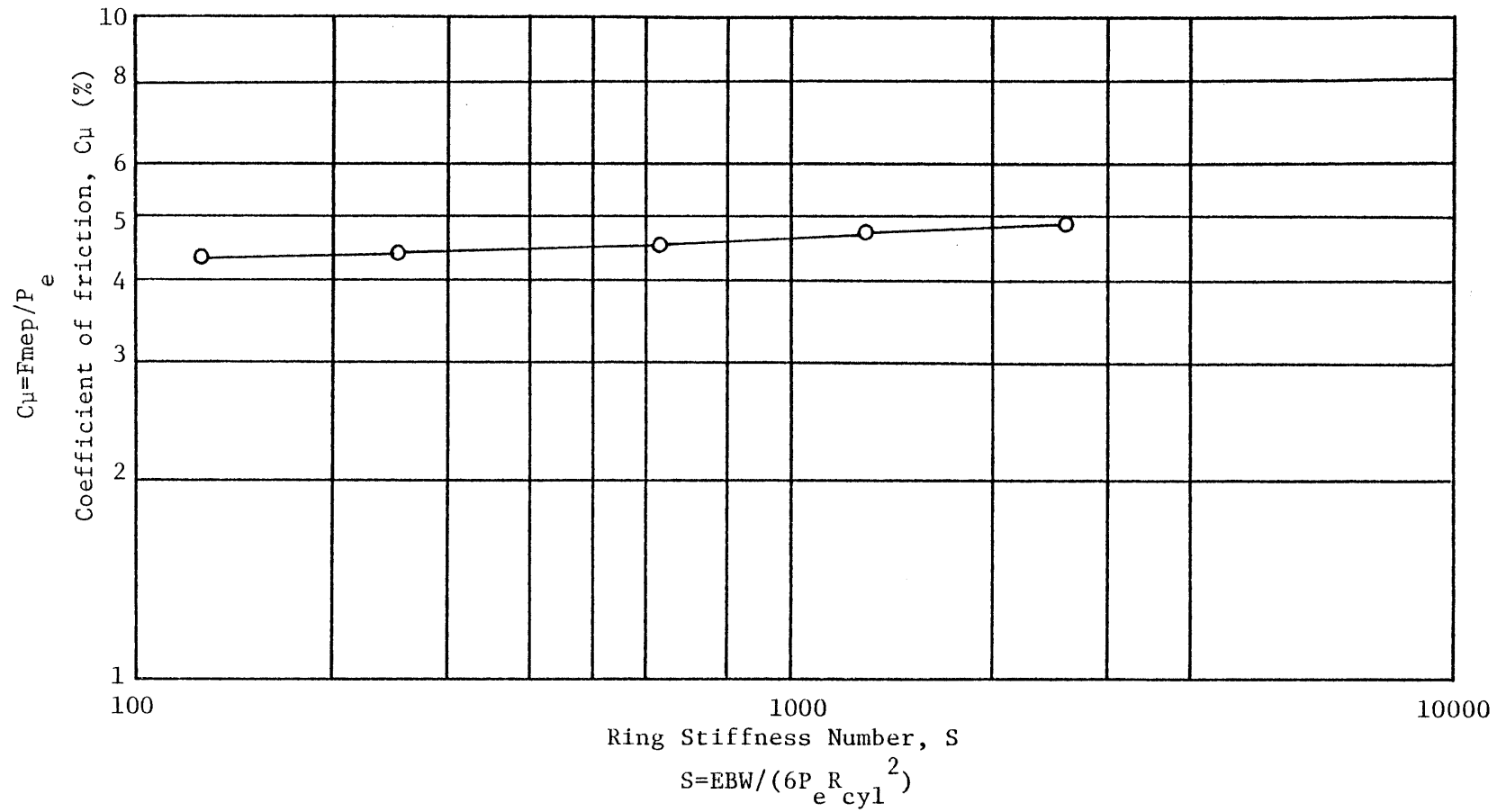


Figure 7.1-2 Coefficient of friction versus ring stiffness number

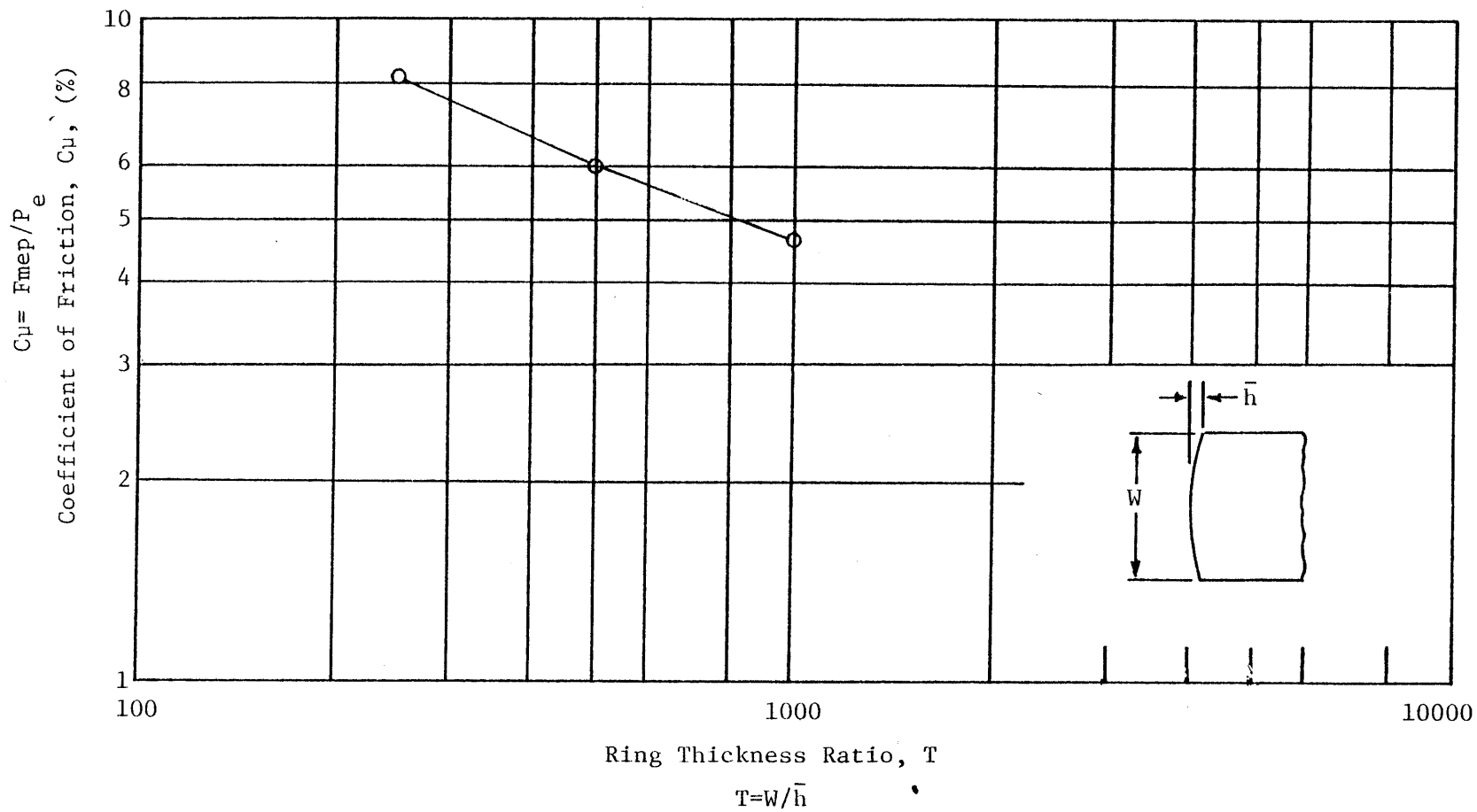


Figure 7.1-3 Coefficient of friction versus ring thickness

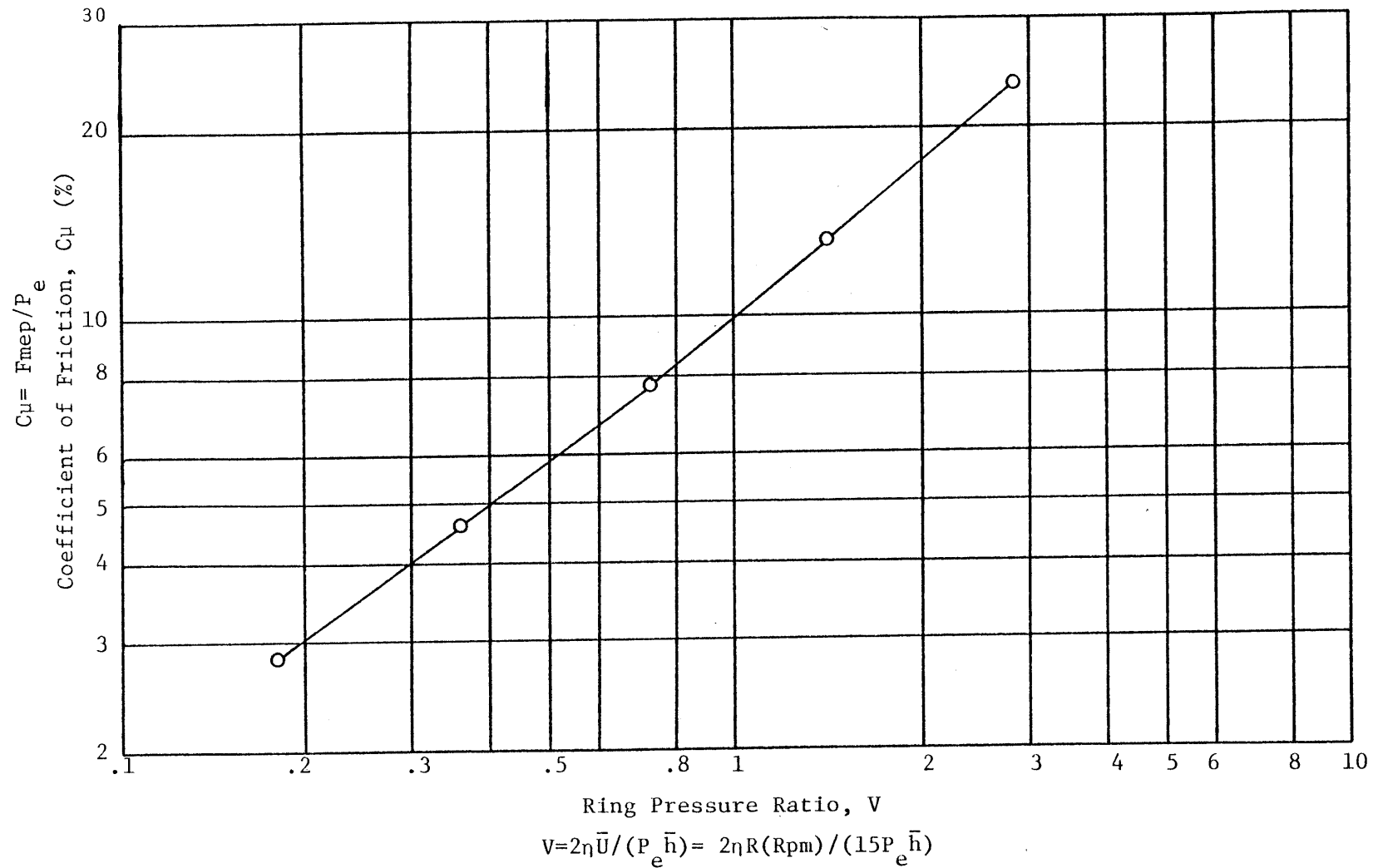
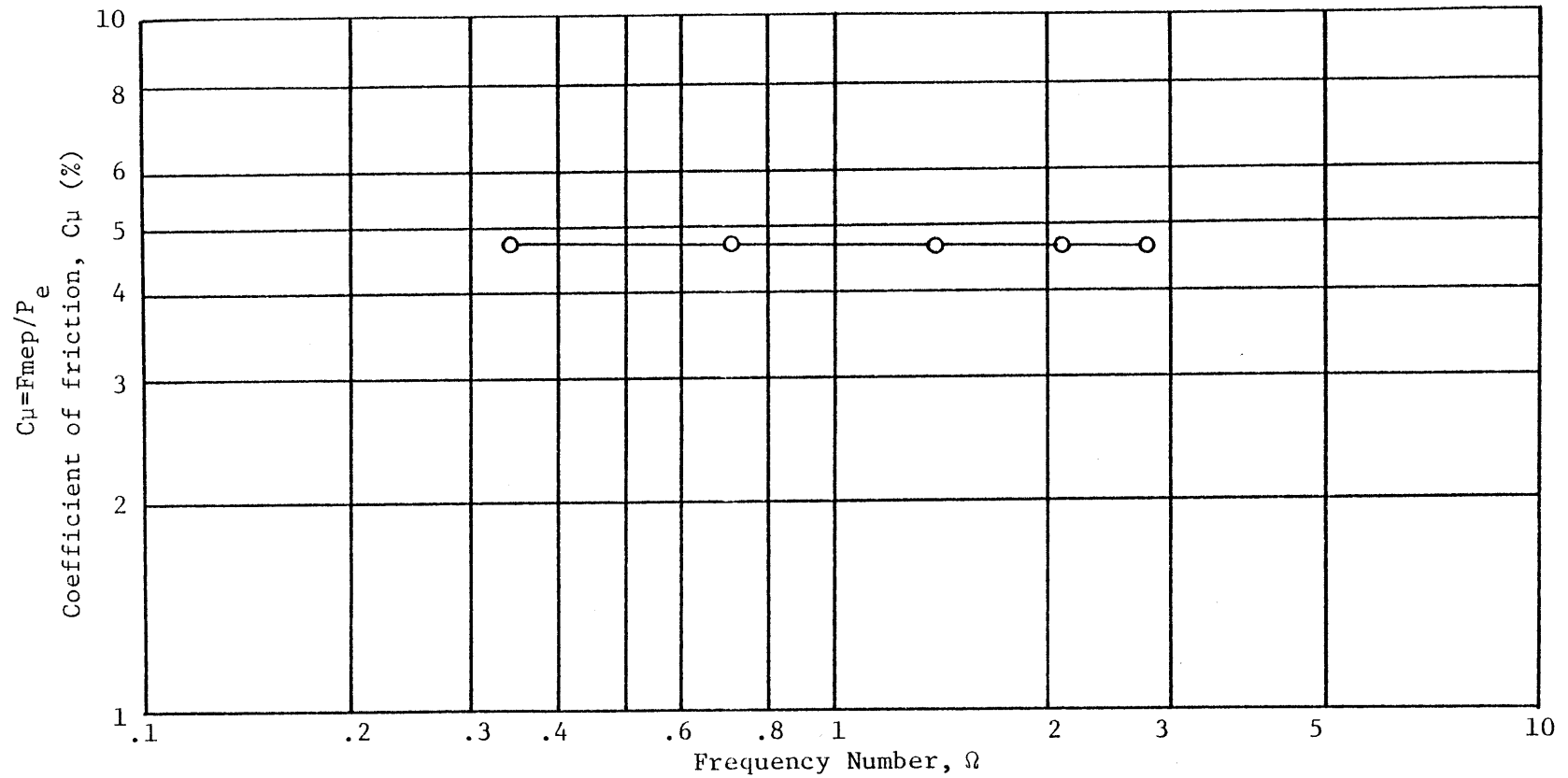


Figure 7.1-4 Coefficient of friction versus ring pressure ratio



$$\Omega = P_e R / (2\rho \bar{U}^2 B) = 225 P_e / (2\rho R B (Rpm)^2)$$

Figure 7.1-5 Coefficient of friction versus frequency number

The effect of the thickness ratio (T) on C_{μ} is approximately from Fig. 7.1-3

$$C_{\mu} = 0.0464 \left[\frac{T^{-0.404}}{1000} \right]$$

Physically, T is the ratio of ring width to the ring profile height, which is the characteristic film height. The inverse of T, which Furuhamma termed ϵ (found statistically to be about 0.001) is a measure of wear on the ring surface forming the surface contour. The larger the value of ϵ , the larger the wear. Also the smaller the value of T, the larger the wear. So, for a heavily worn ring, the friction increased.

This does not mean that a very new surface with a near flat profile has lower friction. Actually, a new ring may have a higher C_{μ} because the surface irregularities have contacted others on the opposing wall across the channel.

The effect of ring pressure ratio (V) on C_{μ} is approximately

$$C_{\mu} = 0.0773 \left[\frac{V^{(0.754 + .1421 \log(V/.725))}}{.725} \right]$$

Physically, V is the ratio of the characteristic shear stress to the ring elastic pressure. As engine speed or viscosity increased the coefficient of friction increases at an exponential rate of about 0.75. Furuhamma⁴ had shown experimentally that the variation

⁴Furuhamma, Takiguchi, Tonizawa, 'Effect of Piston and Piston Ring Design on the Piston Friction Forces in Diesel Engines,' SAE paper no. 810977, p.63.

of friction with Un was exponentially about 0.65.

In Fig. 7.1-5, it is apparent that C_{μ} is almost invariant with Ω . This is the ratio of ring elastic pressure to the average inertial pressure due to piston acceleration. This trend suggests that lighter ring material may not change the friction significantly. The coefficient of friction is about 0.046.

How do the simulation result compare with available physical data? In Millington and Hartles⁵ (1968), the loss per ring was estimated at 3 psi. However, in the simulation reported here, the friction (at $\eta = .0134$, Temp. = 90°C) is about 1.5 times smaller than the empirical estimate. This is to be expected, since the conditions used in the simulation were idealized. The trend of friction increase in the simulation is similar to the experiments.

7.3 State Variable variation

The film height h_r and friction drag, for the standard case, are shown in Fig. 7.3-1. Also, ring tilt angle α and ring axial position are shown in Fig. 7.3-2. Furthermore, the film height and the twist angle are shown in normalized units, each normalized with respect to \bar{h} and $\bar{\alpha}$. In this case \bar{h} is 1.98 μm , and $\bar{\alpha}$ is .4846 minute. The maximum twist angle is $14\bar{\alpha}$.

⁵Millington, B. W. and E. Hartles, 'Frictional Losses in Diesel Engines,' SAE Transactions, paper no. 680590, v.77, 1968.

In Figure 7.3-1, the maximum reference film height is only about 3 μm . The compression stroke and the power stroke both have lower film heights. This contributes to the increase in friction during these two strokes. On the other hand, the exhaust stroke is nearly the mirror image of the intake stroke since this case assumes the cylinder gas pressure to be atmospheric. This film height history corresponds to Rangert's simulation result.

Also, the film does not collapse near the end of each stroke. However, it is very thin at these places, especially near the top dead center position before firing. This may account for the heavy wear on the cylinder wall since the irregularities on the surface may make solid contact with parts of the wall.

The peak in the friction occurs about 30 degrees before TDC caused by the combination of a thin film and relatively high piston speed. The friction near the end of the stroke cannot be determined by this since the film is thin enough for boundary lubrication to occur.

Referring to Fig. 7.3-2, the largest ring tilt occurred just after the TDC following compression. This large ring tilt was necessary to generate the lift force when the piston speed was low. In addition, the pressure difference across the ring during the expansion stroke worked in the same direction to tilt the ring to larger angle.

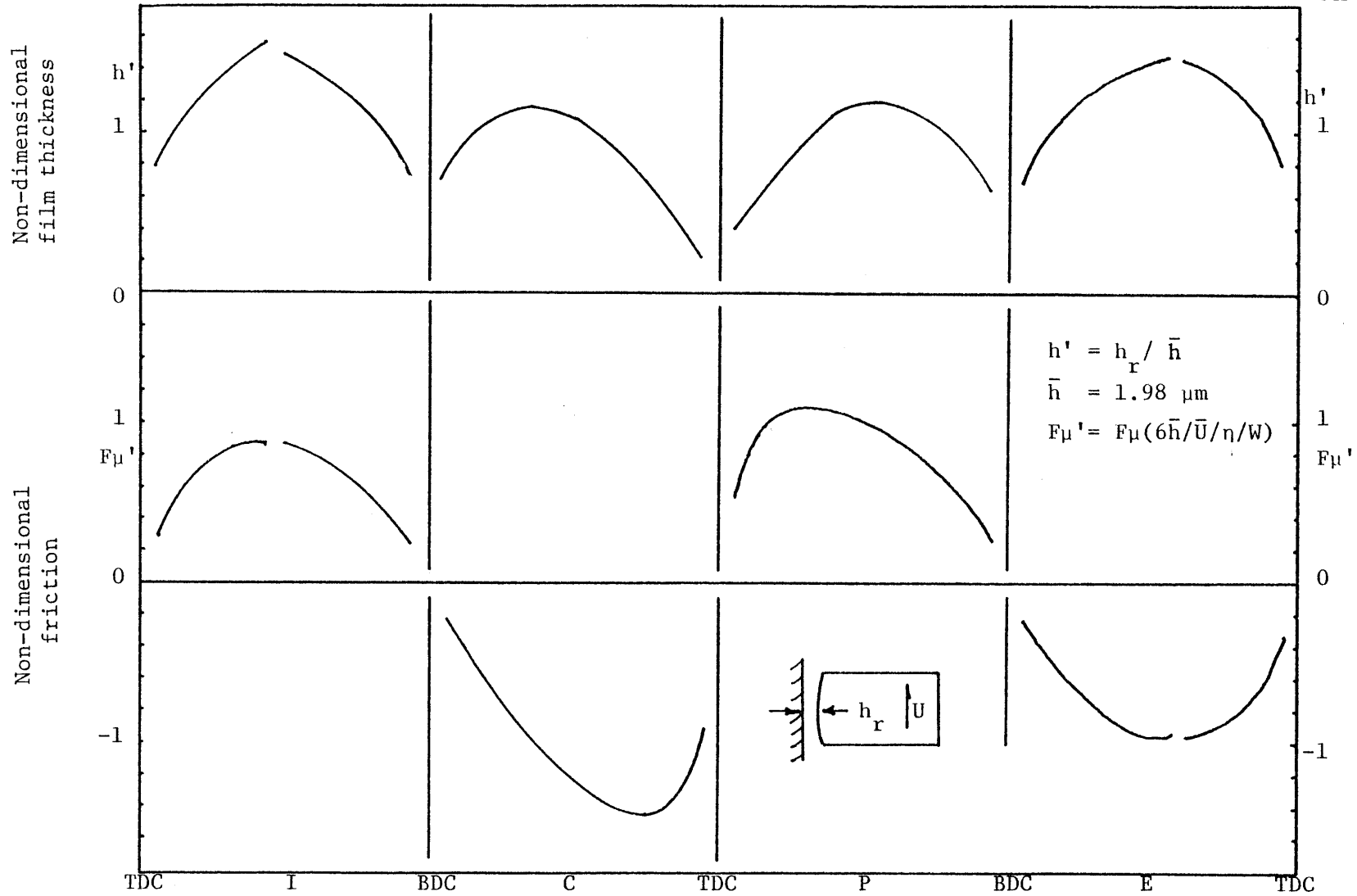


Figure 7.3-1 Film height, h' and friction F_{μ}' versus crank angle

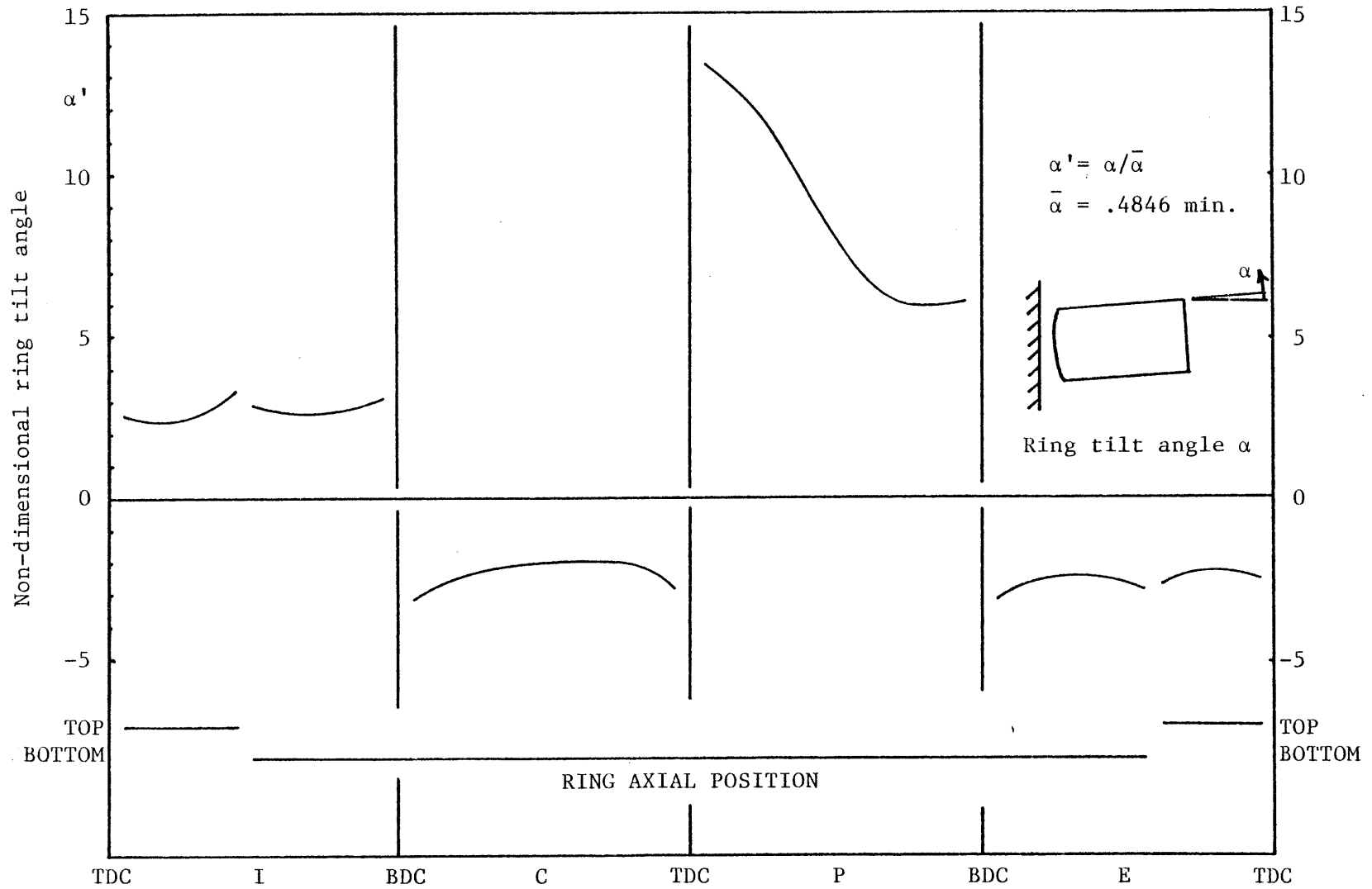


Figure 7.3-2 Ring tilt angle, α' and axial position versus crank angle

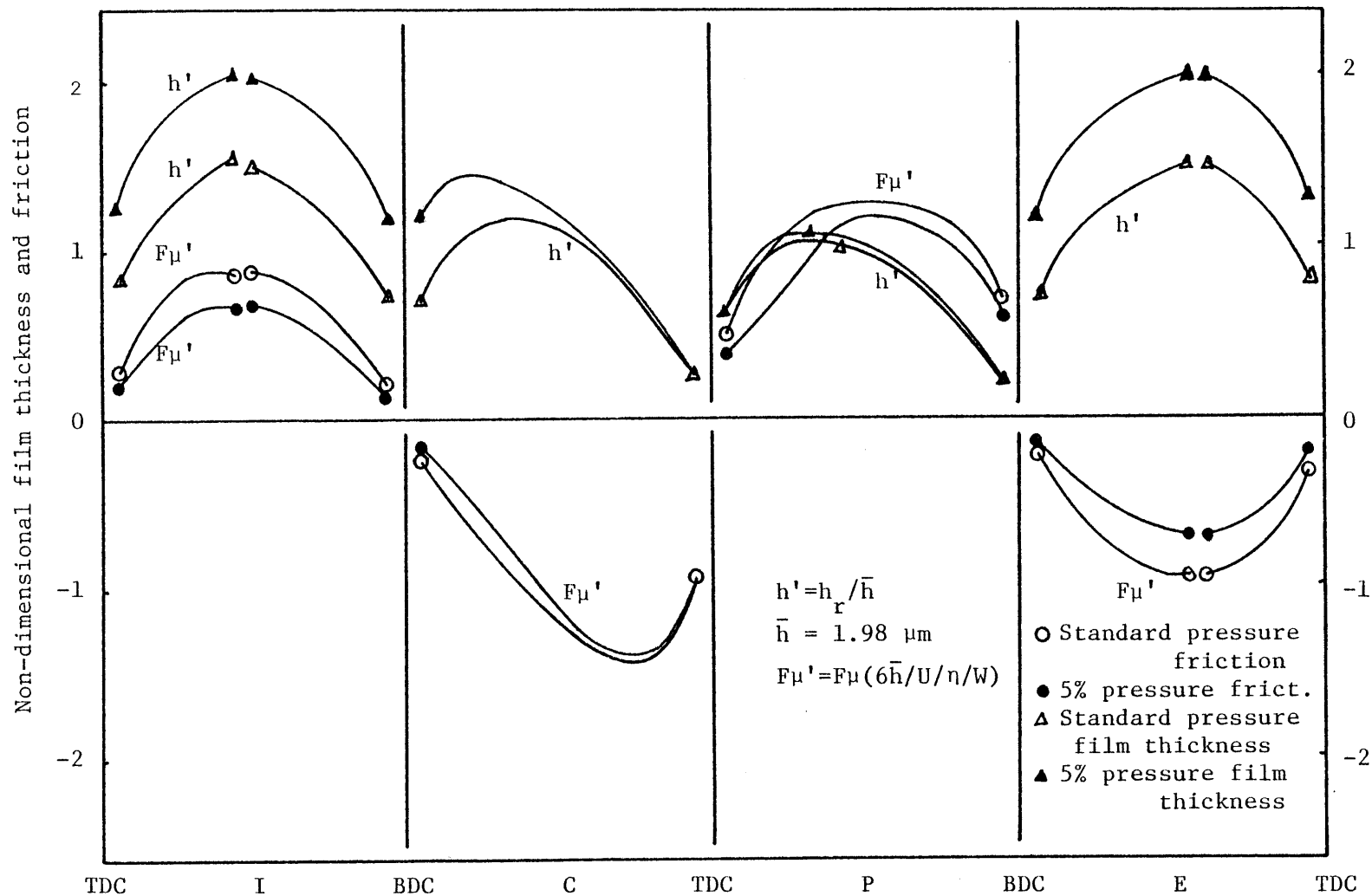


Figure 7.3-3 Effect of lighter ring elastic pressure on oil film thickness and friction

There are six turning points in the cycle. Ring tilt angles change sign at the end of each stroke, and the corresponding film thicknesses vary slightly. In addition, midway through the intake and the exhaust stroke the ring changes its axial position in the ring groove. The film thicknesses and ring tilt angles in these regions are unknown since they are the result of ring transient behavior and the model's quasi-static assumptions are not valid in these regions.

Concerning the effect of ring elastic pressure, it apparently does not have a significant influence on friction, as demonstrated in Figure 7.3-3. The effect of reducing ring pressure to five percent of the standard pressure decreased the Fmep loss from 0.63 psi to 0.54 psi, a fifteen percent change. Therefore, it may not be profitable to reduce ring tension since the loss due to blow by gas may offset the reduction in friction.

CHAPTER 8

Conclusions

Not all terms of the equations used in this three degrees of freedom model need to be taken into consideration during the numerical simulation. It is sufficient, for friction calculation purposes, to take into consideration only the largest terms and the steady state terms. The time variant terms can be neglected because they usually are much smaller than the others. These terms do not contribute significantly to the friction except near the turning points.

There are at least five similarity parameters that dominate the piston ring friction. They correlate the different combinations of ring and piston to friction. By solving one set of similarity solutions, in dimensionless form, the friction loss for a variety of ring and piston combination may be predicted.

Among the five, the most dominant parameter is V , the pressure ratio. This shows that both engine speed and oil viscosity has a very large effect on F_{mep} , a well known fact. To a lesser extent, the ring elastic pressure also matters. From Eq. 7.2-4, this relationship may be approximated by:

$$F_{mep} \propto \left[\frac{2\eta\bar{U}}{h} \right]^{0.75} \cdot [P_e]^{0.25}$$

The effect of ring thickness parameter (T) suggests that an overly worn ring should be replaced since it is likely to have higher friction.

The other three parameters, R, S, and Ω , are less influential. The larger friction from the oil control ring may be inherent in its design, but the aspect ratio does not affect the friction too much. Finally, ring stiffness and inertia seem to have negligible effect upon friction loss.

Many important questions remain to be answered, however. For instance, what are the necessary elements in low friction piston ring design? Does using a low viscosity oil mean better engine performance? What are the necessary design changes to reduce friction? Would lower engine speed result in smaller frictional loss? Would a wider ring be better? What are the sacrifices and tradeoffs in engine wear and lubrication oil consumption rate that these changes lead to? The numerical simulation offers some interesting results, but the answers to the important questions must be left to the design engineers.

REFERENCES

1. Bishop, I. N., 'Effect of Design Variables on Friction and Economy,' Automotive Engineering Congress, Jan. 13-17, 1964. SAE 812A.
2. Cameron, Alastair, Basic Lubrication Theory, 2nd ed., John Wiley and Sons.
3. Furuham, Shoichi, 'Dynamic Theory of Piston Ring Lubrication' JSME Bulletin, v.2, no.7, 1959.
4. Furuham, Shoichi, and Masaru Hiruma, 'The Relationship Between Piston Ring Scuffing and the Formation of Surface Profile,' Proceedings Institution of Mechanical Engineers Conference, C67/75, 1975, pp.35-43.
5. Furuham, S., Masuaki Takiguchi, and Kenji Tonizawa, 'Effect of Piston and Piston Ring Design on the Piston Friction Forces in Diesel Engines,' SAE Paper no.810977.
6. Krauter, Allan I., 'Measurements of Oil Film Thickness for Reciprocating Elastomeric Seals,' D.O.E. Automotive Technology Development Contractor Coordinator Meeting, Nov. 11, 1980. Dearborn, Michigan.
7. Levy, Samuel and W. D. Kroll, 'Errors Introduced by Finite Spaces and Time Increments in Dynamic Response Computation,' Proc., First US National Congress of Applied Mechanics, 1951. pp.1-8.
8. McGeeham, J. A., 'A Literature Review of the Effect of Piston and Ring Friction and Lubricating Oil Viscosity on Fuel Economy,' SAE Transactions, v.87, 1978, Paper no.780673.
9. Millington, B. W. and E. R. Hartles, 'Frictional Losses in Diesel Engines,' Paper no. 680590, SAE Trans., v.77, 1968.
10. Namazian, Mehdi, Studies of Combustion and Crevice gas motion in a flow visualizaition spark-ignition engine, Ph.D. Thesis Massachusetts Institute of Technology, 1981.
11. Purday, H.F.P., Streamline Flow, Constable, 1949. pp.60-62.
12. Rangert, Bo, Hydrodynamic Piston Ring Lubrication with Reference to Lubricating Oil Consumption, Doctoral Thesis, Chalmers University of Technology, Goteburg, Sweden, 1974.
13. Reynold, O., 'Philosophical Transactions of the Royal Society,' (1886) pp.157-243.
14. Wing, R. D. and O. Saunder, 'Oil Film Temperature and Thickness measurements on Piston Rings of a Diesel Engine,' Proceedings Institution of Mechanical Engineers, v.186/172, 1972. pp.1-9.

APPENDIX A1: Effective Slope Model Program (ESMOD) Listing

```

COMMON/CONST1/CONA09,CONA01,CONA04,CONA05,CONA06,CONA07,
1 DELP,PELA,CONA10,CONA11,CONA12,CONA13
COMMON/CONST3/ALPMND,PHIND,ALPHND,CON003,CON002,MODE
COMMON//Y,U,DDY
COMMON /KINDAT/ THTA,DTHTA,DDTHTA,PHE,DPHE,DDPHE
COMMON /CRANK/ AL,R
DIMENSION PSI(100),PCYL(100)
OPEN(UNIT=1,NAME='DATA4.',TYPE='OLD')
OPEN(UNIT=3,NAME='DATA5.',TYPE='NEW')
C READ IN MAIN PROGRAM CONTROL VARIABLES
C   AL   CONNECTING ROD LENGTH IN METERS
C   R    CRANK RADIUS IN METERS
C   RPM  ENGINE SPEED IN REV. PER MIN.
C   RHO  RING DENSITY IN SI UNIT
C   E    RING MODULUS OF ELASTICITY IN PASCALS
C   ETA  OIL DYNAMIC VISCOSITY IN SI UNIT
C   PELA RING ELASTIC PRESSURE IN PASCALS
C   COMPRA COMPRESSION RATIO
READ (1,101) AL,R,RPM,RHO,E,ETA,PELA,COMPRA
101 FORMAT (8F10.2)
C   B    RING RADIAL WIDTH IN mm
C   W    RING AXIAL WIDTH IN mm
C   RCYL CYLINDER RADIUS IN SI
C   ALPCHR CHARACTERISTIC RING TILT ANGLE IN MINUTES
C   HCHR  CHARACTERISTIC FILM HEIGHT IN MICROMETERS
C   RHOIL OIL DENSITY IN SI UNITS
C   ALPMAX MAXIMUM DIMENSIONLESS RING TILT ANGLE
C         IN TERMS OF ALPCHR
C   EPSIL CONVERGENCE CRITERION, USUALLY 0.001
READ (1,101) B,W,RCYL,ALPCHR,HCHR,RHOIL,ALPMAX,EPSIL
C   THESE TWO ARE THE LIMITS FOR ITERATION
READ (1,101) XKAI,XKBI
C   THIS IS THE NUMBER OF PRESSURE POINTS SPECIFIED BY THE PROGRAM
READ (1,103) NHP
103 FORMAT (6I5)
IF (XKAI.LT.XKBI) GO TO 70
T=XKAI
XKAI=XKBI
XKBI=T
70 CONTINUE
C DATA CONVERSION INTO SI UNITS
B=B/1000.
W=W/1000.
ALPCHR=ALPCHR/3437.747
ALPMAX=ALPMAX/3437.747
HCHR=HCHR/1E6
DTHTA=RPM/9.549298
P2=101320.
CLRDIS=2.*R/(COMPRA-1.)
UAVE=R*RPM/15.
ALPMND=ALPMAX/ALPCHR

```

```
IF (HCHR.EQ.0.) HCHR=6.*ETA/UAVE/RHOOIL
IF (ALPCHR.EQ.0.) ALPCHR=2.*PELA*HCHR**3./UAVE/ETA/W/W
```

```
CONA09=6.*ETA/W/ALPCHR/ALPCHR/PELA
CONA01=(B/W)**2/4./PELA
CON003=E*B*W*ALPCHR/6./PELA/RCYL**2
CONA04=RHO*B*B*ALPCHR/PELA/W/ALPMAX
CONA05=12.*ETA/PELA/W/ALPCHR/ALPCHR
CON002=ALPCHR/ALPMAX
CONA06=ETA*B/PELA/W/W/ALPCHR
CONA07=ALPCHR*B/PELA/W
CONA10=3.*HCHR*B/ETA/UAVE/W
CONA11=6.*HCHR*RHO*B/ETA/UAVE
CONA12=6.*HCHR/ALPCHR/UAVE/W
CONA13=6.*HCHR*ALPCHR/ETA/UAVE
```

```
C
C READ IN A FILE OF CRANK ANGLE, AND CYLINDER PRESSURE.
C   PSI(I) - ANGLE OF CRANK SHAFT W/R TO T.D.C.
C   PCYL(I) - CORRESPONDING CYLINDER PRESSURE
C   DO 201 I=1,NHP
C     READ (1,202,ERR=203) PSI(I),PCYL(I)
C CHANGE PSI(I) INTO RADIANS
C   PSI(I)=PSI(I)/57.29578
C   PCYL(I)=PCYL(I)*101320.
C 201 CONTINUE
C 202 FORMAT (2G10.2)

C.....FOR EACH CRANK ANGLE.....
C 300 CONTINUE
C   READ (1,101) THTA
C   THTA=THTA/57.29578
C   IF (THTA.EQ.0.) GO TO 400

C CALCULATE THE KINEMATIC PARAMETERS OF PISTON MOTION.
C   CALL KINETC

C.....CALCULATE THE PRESSURE FOR EACH ANGLE.....
C   DO 50 I=1,NHP
C 50 IF (ABS(PSI(I)-3.141592).LT.0.0001)
C     1 CONST=PCYL(I)*(2.*R+CLRDIS)**1.4

C SPECIAL CASE: INTERPOLATING FOR PRESSURE AT THIS CRANK ANGLE.
C   IF (THTA.GT.3.1415923.AND.THETA.LT.9.42477) GO TO 607
C   IF (THETA.LT.PSI(1)) THETA=THETA+12.56637
C   DO 601 I=1,NHP-1
C   IF (THETA.LT.PSI(I+1).AND.THETA.GE.PSI(I)) GO TO 602
C 601 CONTINUE
C   WRITE (3,604)
C 604 FORMAT (1X,'THETA OUTSIDE THE GIVEN FIELD')
C   GO TO 400
```

```

607 FMULT=1.
   IF (THTA.GT.6.02138.AND.THTA.LT.6.8940505)
1  FMULT=1.+(THTA-6.02138)/0.872665*3.0
   IF (THTA.GT.6.89405) FMULT=4.0
   DISPL=CLRDIS+2.*R-Y
   P1=CONST*FMULT/DISPL**1.4
   GO TO 606

602 CALL INTPOL(PSI(I+1),PSI(I),PCYL(I+1),PCYL(I),THTA,P1)
C.....
606 CONTINUE
   DELP=P1-P2
   TYPE *,THTA*57.29578,P1/101320.,Y,U,DDY
C ASSUME THE RING IS MOVING UPWARD AND IS ON THE BOTTOMLAND
   MODE=3
   IF (U.GT.0.0.AND.FORCND.LT.0.0) MODE=2
   IF (U.LT.0.0.AND.FORCND.GE.0.0) MODE=4
   IF (U.GT.0.0.AND.FORCND.GE.0.0) MODE=1
90  XKA=XKAI
   XKB=XKBI
   MODTST=MODE
C USE SUBROUTINE BISECT TO SOLVE FOR THE RIGHT K VALUE
   CALL BISECT(XKA,XKB,EPSIL,XK,RESIDC)
C USE AXIFOR TO TEST IF THE RING MODE ASSUMPTION IS CORRECT
   CALL AXIFOR(XK,FORCND,FMUND)
C IF THE MODE IS WRONG, CHANGE A MODE.
   IF (MODTST.NE.MODE) GO TO 90
   HRND=ALPCHR*W*PHIND/HCHR/XK
   WRITE (3,605) THTA*57.29578,DELP/101320.,HRND,PHIND,ALPHND,FMUND,
1  Y,U,DDY,XK,MODE
C OUTPUT THE DATA INTO DATA FILE
   TYPE *,XK,RESIDC,HRND,PHIND,ALPHND,FMUND,MODE
   TYPE *,'...'
605 FORMAT (1X,10(1X,G10.4),I2)
   GO TO 300
400 CLOSE (UNIT=3)
   CLOSE (UNIT=1)
203 STOP
   END

```

SUBROUTINE AXIFOR(XK,FORCND,FMUND)

```

C-----
COMMON //Y,U,DDY
COMMON/CONST3/ALPMND,PHIND,ALPHND,CON003,CON002,MODE
COMMON/CONST1/CONA09,CONA01,CONA04,CONA05,CONA06,CONA07,
1  DELP,PELA,CONA10,CONA11,CONA12,CONA13
   XK1=XK+1.
   XK2=XK+2.
   FMUND=CONA12*U/PHIND*LOG(XK1)+CONA13*DELP*PHIND*XK1/XK2/XK
C CALCULATE NET FORCE ACTED BY PISTON ON RING
   IF (MODE.EQ.1) GO TO 40
   IF (MODE.EQ.2) GO TO 30
   IF (MODE.EQ.3) GO TO 20

```

```

C MODE 4. RING AT BOTTOM, U<0, MOVING DOWN.
  FORCND=CONA10*DELP*(1.+CON002*(ALPMND-PHIND))+CONA11*DDY+FMUND
  IF (FORCND.LT.0.0) GO TO 11
  RETURN
11 MODE=3
  RETURN
C MODE 3. RING AT TOP, U<0, MOVING DOWN.
  20 FORCND=CONA10*DELP*(1.-CON002*(ALPMND-PHIND))+CONA11*DDY+FMUND
  IF (FORCND.GT.0.0) GO TO 21
  RETURN
21 MODE=4
  RETURN
C MODE 2. RING AT TOP, U>0, MOVING UP.
  30 FORCND=CONA10*DELP*(1.+CON002*(ALPMND-PHIND))+CONA11*DDY+FMUND
  IF (FORCND.GT.0.0) GO TO 31
  RETURN
31 MODE=1
  RETURN
C MODE 1. RING AT BOTTOM, U>0, MOVING UP.
  40 FORCND=CONA10*DELP*(1.-CON002*(ALPMND-PHIND))+CONA11*DDY+FMUND
  IF (FORCND.LT.0.0) GO TO 42
  RETURN
42 MODE=2
  RETURN
  END

```

SUBROUTINE BISECT(XKA,XKB,EPSIL,C,RESIDC)

```

C-----
COMMON/CONST2/CON009,CON008,CON001,CON004,CON005,CON006,CON007
COMMON/CONST3/ALPMND,PHIND,ALPHND,CON003,CON002,MODE
COMMON/CONST1/CONA09,CONA01,CONA04,CONA05,CONA06,CONA07,DELP,PELA
1 ,CONA10,CONA11,CONA12,CONA13
COMMON //Y,U,DDY

CON009=CONA09*U
CON008=DELP/PELA
CON001=DELP*CONA01
CON004=CONA04*DDY
CON005=CONA05*U
CON006=CONA06*U
CON007=DELP*CONA07
T=2.*ALPMND
C SEE TEXAS INSTRUMENTS SOFTWARE MODUAL NO.1 FOR TI-58 CALCULATORS.
A=XKA
CALL XKPHI(A,RESIDA)

50 IF (A.GE.XKB) GO TO 30
  B=A+1.0
  CALL XKPHI(B,RESIDB)

10 IF (ABS(A-B).LT.EPSIL) GO TO 60
  C=(A+B)/2.
  CALL XKPHI(C,RESIDC)
  IF ((RESIDA*RESIDB).GT.0.0) GO TO 40

```



```

IF ((RESIDA*RESIDC).LT.0.0) GO TO 20
A=C
RESIDA=RESIDC
GO TO 10

```

```

20 B=C
RESIDB=RESIDC
GO TO 10

```

```

40 A=B
RESIDA=RESIDB
GO TO 50

```

```

60 IF (PHIND.GT.T.OR.PHIND.LT.0.0) GO TO 40
RETURN

```

```

30 WRITE (5,31) XKA,RESIDA,XKB,RESIDB,XKC,RESIDC
31 FORMAT (1X,'THE RESIDUES HAVE THE SAME SIGNS... ',/,6(1X,G10.4))
STOP
END

```

```

SUBROUTINE XKPHI(XK,FPHI)

```

```

C-----
C THIS SUBROUTINE CALCULATES FOR THE RESIDUE OF RADIAL FORCE BALANCE
DOUBLE PRECISION XK,XK1,XK2
COMMON/CONST2/CON009,CON008,CON001,CON004,CON005,CON006,CON007
COMMON/CONST3/ALPMND,PHIND,ALPHND,CON003,CON002,MODE
XK1=XK+1.
XK2=XK+2.
IF (MODE.EQ.1) GO TO 10
IF (MODE.EQ.2) GO TO 20
IF (MODE.EQ.3) GO TO 30
C MODE 4 OPERATION: U<0, RING AT BOTTOM LAND
PHIND=SQRT(-CON009*(LOG(XK1)-2.*XK/XK2)/(1.+CON008*XK1/XK2))
FPHI=CON001*(1.+CON002*(ALPMND-PHIND))**2.+1.
1 +(CON003+CON004)*(ALPMND-PHIND)
2 +CON005/PHIND**2*(LOG(XK1)-2.*XK/XK2)*(2.*(XK2+1.)*XK1*LOG(XK1)
3 -XK*(6.+5.*XK))/2./XK/(XK2*LOG(XK1)-2.*XK)
4 +CON008*2.*XK1*XK1/XK/XK/XK2*((XK-2.)/2.+LOG(XK1)/XK)
5 +(1.+CON002*(ALPMND-PHIND))*(CON006/PHIND*LOG(XK1)+CON007
6 *PHIND/XK*XK1/XK2)
ALPHND=PHIND-ALPMND
RETURN
C MODE 3 OPERATION: U<0, RING AT TOP LAND.
30 PHIND=SQRT(-CON009*(LOG(XK1)-2.*XK/XK2))
FPHI=-1.+(CON003-CON004)*(ALPMND-PHIND)+2.*(1.-(2.*(3.+XK)*XK1*LOG
1 (XK1)-XK*(6.+5.*XK))/(2.*XK*(XK2*LOG(XK1)-2.*XK)))
2 +CON006/PHIND*(1.-CON002*(ALPMND-PHIND))*LOG(XK1)
ALPHND=PHIND-ALPMND
RETURN
C MODE 2 OPERATION: RING AT TOP LAND, U>0.
20 PHIND=SQRT(CON009*(LOG(XK1)-2.*XK/XK2))
FPHI=-1.-(CON003-CON004)*(ALPMND-PHIND)
1 +2.*(2.*(XK+3.)*XK1*LOG(XK1)-XK*(6.+5.*XK))/(2.*XK*(XK2*

```

```

2 LOG(XK1)-2.*XK))+CON006*(1.+CON002*(ALPMND-PHIND))/PHIND*LOG(XK1)
ALPHND=ALPMND-PHIND
RETURN

```

```

C MODE 1 OPERATION: RING AT BOTTOM, U>0.

```

```

10 PHIND=SQRT(CON009*(LOG(XK1)-2.*XK/XK2)/(1.+CON008/XK2))
    FPHI=CON001*(1.-CON002*(ALPMND-PHIND))**2.+1.-(CON003+CON004)*
1 (ALPMND-PHIND)-CON005/PHIND/PHIND*(LOG(XK1)-2.*XK/XK2)*(1.-
2 (2.*(XK+3.)*XK1*LOG(XK1)-XK*(6.+5.*XK))/(2.*XK*(XK2*LOG(XK1)-
3 2.*XK)))+(1.-CON002*(ALPMND-PHIND))*(CON006/PHIND*LOG(XK1)+
4 CON007*PHIND*XK1/XK/XK2)+CON008*(1.-2.*XK1*(XK1*(0.5/XK/XK-
5 LOG(XK1)/XK/XK/XK/XK2)-1./XK/XK2))
ALPHND=ALPMND-PHIND
RETURN
END

```

SUBROUTINE KINETC

```

C-----THIS SUBROUTINE SOLVES FOR THE VELOCITY AND ACCELERATION
C OF THE PISTONS-----

```

```

COMMON // Y,DY,DDY
COMMON /KINDAT/ THTA,DTHTA,DDHTA,PHI,DPHI,DDPHI
COMMON /CRANK/ AL,R

```

```

C AL =LENGTH OF CONNECTING ROD
C R =CRANK RADIUS OF ROTOR
C THTA =ANGLE OF ROTOR FROM TDC OF COMBUSTION
C DTHTA =SPEED OF ROTOR
C DDHTA=ANGULAR ACCELERATION OF ROTOR
C PHI =ANGLE OF CONNECTING ROD RELATIVE TO CENTERLINE
C DPHI =SPEED OF CHANGE OF PHI
C DDPHI =SPEED OF CHANGE OF DPHI
C Y =POSITION OF PISTON, COMPRESSION MOVEMENT BEING POSITIVE
C DY =VELOCITY OF PISTON, COMPRESSION MOVEMENT BEING POSITIVE
C DDY =ACCELERATION OF PISTON

```

```

C CALCULATE VARIABLES

```

```

STHTA=SIN(THTA)
CTHTA=COS(THTA)
RATIO=R/AL
PHI =ASIN(RATIO*STHTA)
CPHI =COS(PHI)
SPHI =SIN (PHI)
Y =R*CTHTA+AL*CPHI-AL+R
DPHI =DTHTA*RATIO*CTHTA/CPHI
DY =-(DTHTA*R*STHTA+DPHI*AL*SPHI)
DDPHI=DDHTA*RATIO*CTHTA/CPHI+DPHI**2.*TAN(PHI)-DTHTA**2.
1 *RATIO*STHTA/CPHI
DDY =-(DDHTA*R*STHTA+DTHTA**2.*R*CTHTA+
1 DDPHI*AL*SPHI+DPHI**2.*AL*CPHI)
RETURN
END

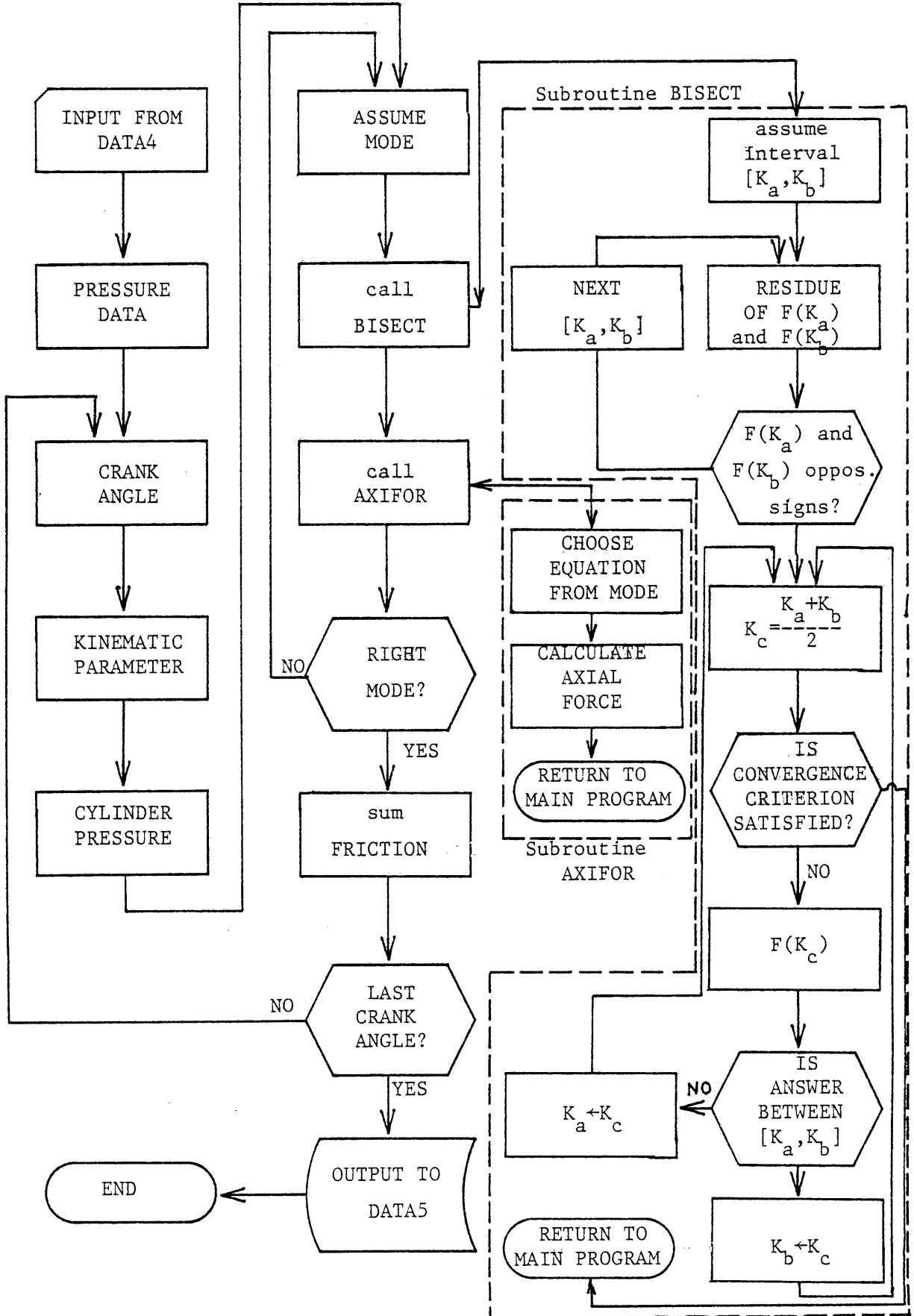
```

SUBROUTINE INTPOL(X2,X1,Y2,Y1,X,Y)

```

C-----THIS IS USED TO INTERPOLATE FOR GAS PRESSURE-----
Y=Y1+(Y2-Y1)/(X2-X1)*(X-X1)
RETURN
END

```



APPENDIX A3: DATA4 Input Format Sample

0.2286	0.0492	3000.	7900.	2.05E11	.0033594	93586.
8.0						
4.293	1.981	0.0500	0.4846	2.93	700.	16.0
0.001						
0.01	50.0					
004						
000.	1.					
180.	1.					
540.	1.					
720.	1.					
10.						
20.						
30.						
40.						
50.						
60.						
.						
.						
.						
690.						
700.						
710.						
0.						

0.2286	connection rod length in m
0.0492	crank radius in m
3000.	engine rpm
7900.	ring density in Kg/m ³
2.05E11	ring modulus of elasticity in Pa
.003359	oil viscosity in Pa-s
93586.	ring elastic pressure
8.0	compression ratio
4.293	ring radial width in mm
1.981	ring axial width in mm
0.05	cylinder radius in m
0.4846	characteristic ring tilt angle in minutes
2.93	characteristic film height in μ m
700.	oil density in Kg/m ³
16.	maximum N-D ring tilt angle
0.001	convergence criterion
0.01	minimum K, K _a
5.0	maximum K, K _b
004	Four pressure data points following...
10.-0.	Crank angles to evaluate

APPENDIX A4: DATA5 Output Format Sample

CR Angle	$\Delta P(\text{atm})$	h'	ϕ'	α'	F_{μ}'	Y	U	acc.	K	mode
10.00	0.0000	2.057	19.63	-.3720	-.6859	0.9749E-01	-3.253	-5766.	0.9094	3
20.00	0.0000	2.779	19.62	-.3775	-1.067	0.9481E-01	-6.359	-5371.	0.6731	3
.
.
.
170.0	0.0000	1.674	19.47	-.5251	-.5183	0.5877E-03	-2.115	3798.	1.109	4
190.0	0.7363E-02	1.672	19.45	0.5500	0.5196	0.5877E-03	2.115	3798.	1.109	1
200.0	0.2997E-01	2.302	19.42	0.5842	0.8228	0.2347E-02	4.214	3755.	0.8039	1
.
.
.
690.0	0.0000	3.250	19.62	0.3792	1.360	0.9048E-01	9.177	-4740.	0.5754	2
700.0	0.0000	2.779	19.62	0.3774	1.067	0.9481E-01	6.359	-5371.	0.6731	2
710.0	0.0000	2.057	19.58	0.4172	0.6864	0.9749E-01	3.253	-5766.	0.9075	2
IMEP = 116.3		FMEP = 0.1658								
RPM = 3000.		ALPMND = 20.00								

APPENDIX B1: Composit Secant Model Program (COMSEC) Listing

```

COMMON/CONST1/C1,C2,C3,C4,C5,C6,C7,C8,C9,Q1,Q2
COMMON/CONST2/C10,C11,C12,C13,C14,C15,C16
COMMON/CONST3/C17,C18,C19,C20,C21
COMMON/CONST4/HRNDA,HRNDB,EPSIL,EPSILA,XALPHA,XALPHB,STEP
COMMON/CONST5/ MODE
COMMON//Y,U,DDY
COMMON /KINDAT/ THTA,DTHTA,DDTHTA,PHE,DPHE,DDPHE
COMMON /CRANK/ AL,R
DIMENSION PSI(100),PCYL(100)
OPEN(UNIT=1,NAME='DATA7.',TYPE='OLD')
OPEN(UNIT=3,NAME='DATA8.',TYPE='NEW')
C READ IN MAIN PROGRAM CONTROL VARIABLES
C   AL      CONNECTING ROD LENGTH IN SI
C   R      CRANK RADIUS IN SI
C   RPM     ENGINE R.P.M.
C   RHO     DENSITY OF RING MATERIAL IN SI
C   E      MODULUS OF ELASTICITY OF RING MATERIAL
C   ETA     AVERAGE OIL VISCOSITY IN SI
C   PELA    ELASTIC PRESSURE THAT THE RING EXERTS ON THE WALL
C   COMPRA  COMPRESSION RATIO (VOLUME)
C   READ (1,101) AL,R,RPM,RHO,E,ETA,PELA,COMPRA
101  FORMAT (8G10.2)
C   B      RING RADIAL WIDTH
C   W      RING AXIAL WIDTH IN MM
C   RCYL    RING AND CYLINDER RADIUS IN SI
C   ALPCHR  CHARACTERISTIC RING TILT ANGLE IN MINUTES
C   HCHR    CHARACTERISTIC FILM HEIGHT IN MICROMETERS
C   RHOIL   DENSITY OF OIL IN SI
C   ALPMND  MAXIMUM NON-DIMENSIONAL RING TILT ANGLE
C   EPSIL   FILM HEIGHT CONVERGENCE CRITERION:  USUALLY 0.01
C   READ (1,101) B,W,RCYL,ALPCHR,HCHR,RHOIL,ALPMND,EPSIL
C   HRNDA
C   HRNDB
C   Q1      NON-DIM. CREST POSITION OF RING CONTOUR
C   DELH1   RING TOP PROFILE HEIGHT
C   DELH2   RING BOTTOM PROFILE HEIGHT
C   EPSILA  ANGLE CONVERGENCE CRITERION:  USUALLY 0.001
C   READ (1,101) HRNDA,HRNDB,Q1,DELH1,DELH2,EPSILA
C   NHP     NUMBER OF PRESSURE POINTS SPECIFIED IN DISCRETE FORM
C   READ (1,103) NHP
103  FORMAT (6I5)
C   IF (HRNDA.LT.HRNDB) GO TO 80
C   T=HRNDA
C   HRNDA=HRNDB
C   HRNDB=T
80  CONTINUE

C DATA CONVERSION INTO SI UNITS
W=W/1000.
Q1=Q1*W
B=B/1000.
Q2=W-Q1

```

```

DELH1=DELH1/1.E6
DELH2=DELH2/1.E6
ALPCHR=ALPCHR/3437.747
HCHR=HCHR/1E6
DTHTA=RPM/9.549298
P2=101320.
CLRDIS=2.*R/(COMPRA-1.)
UAVE=R*RPM/15.

```

```

IF (HCHR.EQ.0.) HCHR=6.*ETA/UAVE/RHOOIL
IF (ALPCHR.EQ.0.) ALPCHR=12.*PELA*HCHR**3./UAVE/ETA/W/W
IF (ALPMND.EQ.0.0) ALPMND=HCHR/(W/2)/ALPCHR
ALPMAX=ALPMND*ALPCHR

```

```

C1A=6.*ETA*Q1**2/PELA/W/HCHR/HCHR
C3=Q2/Q1
C4=DELH1/HCHR
C5=ALPCHR*Q1/HCHR
C6=DELH2/HCHR
C7=ALPCHR*Q2/HCHR
C8A=HCHR*HCHR/6./ETA
C9=W/2.
C10A=B*B/W/W/4./PELA
C11=ALPCHR/ALPMAX
C12=E*B*W*ALPCHR/6./PELA/RCYL**2
C13A=RHO*B*B/PELA/W*C11
C14A=Q1*ETA*B/PELA/W/W/HCHR
C15A=2.*Q2/W
C16A=2.*Q1/W
C17A=Q1/W/UAVE
C18A=Q2/W/UAVE
C19A=B*HCHR/2./ETA/W/UAVE
C20=ETA*W/HCHR*UAVE
C21A=RHO*B*HCHR/ETA/UAVE

```

```

C
C READ IN A FILE OF CRANK ANGLE, AND CYLINDER PRESSURE.
C   PSI(I) - ANGLE OF CRANK SHAFT W/R TO T.D.C.
C   PCYL(I) - CORRESPONDING CYLINDER PRESSURE
C   DO 201 I=1,NHP
C     READ (1,202,ERR=203) PSI(I),PCYL(I)
C CHANGE PSI(I) INTO RADIANS
C   PSI(I)=PSI(I)/57.29578
C   PCYL(I)=PCYL(I)*101320.
201 CONTINUE
202 FORMAT (2G10.2)

```

```

C CALCULATE SIMILARTY PARAMETER VALUES
C   AR=B/2/W
C   S=E*B*W/6./PELA/RCYL**2
C   T=W/HCHR
C   V=2.*ETA*UAVE/PELA/HCHR
C   OMEGA=PELA*R/2./RHO/UAVE**2/B
C   TYPE *,AR,S,T,V,OMEGA

```

```

C.....FOR EACH CRANK ANGLE.....
  300 CONTINUE
      READ (1,101) THTA
      THTA=THTA/57.29578
      IF (THTA.EQ.0.) GO TO 400

C CALCULATE THE KINEMATIC PARAMETERS OF PISTON MOTION.
  CALL KINETC

C.....

      DO 605 I=1,NHP
  605 IF (ABS(PSI(I)-3.141592).LT.0.0001)
      1 CONST=PCYL(I)*(2.*R+CLRDIS)**1.4

C SPECIAL CASE: INTERPOLATING FOR PRESSURE AT THIS CRANK ANGLE.
C.....
      IF (THTA.GT.3.1415923.AND.THTA.LT.9.42477) GO TO 607
      IF (THTA.LT.PSI(1)) THTA=THTA+12.56637
      DO 601 I=1,NHP-1
      IF (THTA.LT.PSI(I+1).AND.THTA.GE.PSI(I)) GO TO 602
  601 CONTINUE
      WRITE (3,604)
  604 FORMAT (1X,'THETA OUTSIDE THE GIVEN FIELD')
      GO TO 400

  607 FMULT=1.
      IF (THTA.GT.6.02138.AND.THTA.LT.6.8940505)
  1 FMULT=1.+(THTA-6.02138)/0.872665*3.0
      IF (THTA.GT.6.89405) FMULT=4.0
      DISPL=CLRDIS+2.*R-Y
      P1=CONST*FMULT/DISPL**1.4
      GO TO 606

  602 CALL INTPOL(PSI(I+1),PSI(I),PCYL(I+1),PCYL(I),THTA,P1)
C.....
  606 CONTINUE
      DELP=P1-P2
      TYPE *,THTA*57.29578,P1/101320.,Y/2/R,U,DDY

      IF (U.GT.0.) GO TO 120
      XALPHA=0.01
      XALPHB=ALPMND*.99
      GO TO 121
  120 XALPHA=-.99*ALPMND
      XALPHB=-.01
  121 CONTINUE
      STEP=ABS(XALPHA-XALPHB)/ALPMND

      C1=C1A*U
      C2=DELP/PELA
      C8=C8A*DELP/U
      C10=C10A*DELP
      C13=C13A*DDY

```



```

C14=C14A*U
C15=C15A*C1
C16=C16A*C1
C17=C17A*U
C18=C18A*U
C19=C19A*DELP
C21=C21A*DDY

C ASSUME RING IS AT THE BOTTOM OF THE RING GROOVE
  MODE=1
  IF (FORCND.LT.0.0) MODE=2
  90 CONTINUE
  MODTST=MODE
C USE BISALP TO ITERATE FOR THE RIGHT RING TILT ANGLE
  CALL BISALP(ALPHND,HRND)
C USE AXIFOR TO CHECK IF THE MODE ASSUMPTION IS CORRECT
  CALL AXIFOR(ALPHND,HRND,FMUND)
  IF (MODTST.NE.MODE) GO TO 90
C OUTPUT THE DATA INTO DATA FILE
  WRITE (3,102) THTA*57.29578,DELP/101320.,HRND,ALPHND,FMUND,
  1Y,Y/2/R,U,DDY,MODE
  TYPE *,HRND,ALPHND,FMUND,MODE
  TYPE *,'...'
  102 FORMAT (1X,8(1X,G10.4),I2)
C SUM THE FRICTIONAL LOSS
  DELY=(Y-OLDY)/2/R
  SFRIND=SFRIND+DELY*FMUND
  OLDY=Y
  IF (THTA.GT.3.141592.AND.THETA.LT.9.42477)
  1 FIMEP=FIMEP-DELP*DELY*2*R
  GO TO 300
C CALCULATE THE Imep AND THE Fmep DURING THE CYCLE
  400 FMEP=2.*SFRIND*UAVE*ETA*W/HCHR/RCYL
  FIMEP=FIMEP/2./R*14.7/101320.
  FRICOE=FMEP/PELA
  FMEP=FMEP/101320.*14.7
  WRITE (3,104) FIMEP,FMEP,SFRIND,FRICOE
  104 FORMAT (1X,'IMEP = ',G10.4,' FMEP = ',G10.4,' SFRIND = ',G10.4,
  1 ' FRICOE = ',G10.4)
  TYPE *,'IMEP = ',FIMEP,' FMEP = ',FMEP,' SFRIND = ',SFRIND,
  1 ' FRICOE = ',FRICOE
  WRITE (3,105) RPM,ALPMND,ETA
  105 FORMAT (1X,'RPM = ',G12.4,' ALPMND = ',G12.4,' VISCOSITY = ',
  1 G12.6)
  WRITE (3,101) AL,R,RPM,RHO,E,ETA,PELA,COMPRA
  WRITE (3,101) B,W,RCYL,ALPCHR,HCHR,RHOOIL,ALPMND,EPSIL
  WRITE (3,101) HRNDA,HRNDB,Q1,DELH1,DELH2,EPSILA
  WRITE (3,106) AR,S,T,V,OMEGA
  106 FORMAT (1X,'AR = ',G10.4,' S = ',G10.4,' T = ',G10.4,
  1/,1X,' V = ',G10.4,' OMEGA = ',G10.4)
  WRITE (5,106) AR,S,T,V,OMEGA
  CLOSE (UNIT=3)
  CLOSE (UNIT=1)
203 STOP

```

END

SUBROUTINE BISALP(C,HRNDCC)

```

C-----
C   FOR THE GIVEN RING TILT ANGLE, CALCULATE THE PROPER
C   FILM HEIGHT THAT BALANCES THE RADIAL FORCE.  FOR DETAILS,
C   SEE TEXAS INSTRUMENT SOFTWARE PACKAGE FOR TI-58 CALCULATOR
C.....
COMMON/CONST4/HRNDA,HRNDB,EPSIL,EPSILA,ALPNDA,ALPNDB,STEP

A=ALPNDA
CALL BISHR(HRNDA,HRNDB,EPSIL,A,HRNDCA,RESICA,IFLAGA)
CALL MOMENT(HRNDCA,A,XMOMTA)

C IF THE VARIABLE HAS EXHAUSTED ALL THE INTERVALS...
50 IF (A.GE.ALPNDB) GO TO 30
   B=A+STEP
   IF (B.GT.ALPNDB) GO TO 70
51 CALL BISHR(HRNDA,HRNDB,EPSIL,B,HRNDCB,RESICB,IFLAGB)
   CALL MOMENT(HRNDCB,B,XMOMTB)

C IF THE SOLUTION HAS CONVERGED TO A SMALL INTERVAL...GET OUT
10 IF (ABS(A-B).LT.EPSIL) GO TO 60
   C=(A+B)/2.
   CALL BISHR(HRNDA,HRNDB,EPSIL,C,HRNDCC,RESICC,IFLAGC)
   CALL MOMENT(HRNDCC,C,XMOMTC)

   AB=ABS(XALPHA-XALPHB)
   AC=ABS(XALPHA-XALPHC)
   BC=ABS(XALPHB-XALPHC)
   IF ((BC.GT.AB).OR.(AC.GT.AB)) GO TO 40

   IF ((XMOMTA*XMOMTB).GT.0.0.OR.(IFLAGA.EQ.0.AND.IFLAGB.EQ.0))
1 GO TO 40
   IF ((XMOMTA*XMOMTC).LT.0.0) GO TO 20
   A=C
   XMOMTA=XMOMTC
   GO TO 10

20 B=C
   XMOMTB=XMOMTC
   GO TO 10

40 A=B
   XMOMTA=XMOMTB
   GO TO 50

C IF THE PHYSICAL SOLUTION IS IMPOSSIBLE... STOP IT
60 IF (C.GT.ALPNDB.OR.C.LT.ALPNDA) GO TO 40
   RETURN

30 WRITE (5,31) A,XMOMTA,B,XMOMTB,C,XMOMTC

```

```

WRITE (3,31) A,XMOMTA,B,XMOMTB,C,XMOMTC
31 FORMAT (1X,'THE MOMENT RESIDUE HAVE THE SAME SIGN',
1/,6(1X,G10.4))
STOP
70 B=ALPNDB
GO TO 51
END

```

SUBROUTINE MOMENT (HRND,ALPHND,XMOMNT)

```

C-----
C      GIVEN THE RING TILT ANGLE AND FILM HEIGHT, CALCULATE THE
C      CORRESPONDING MOMENT RESIDUE
C.....
COMMON/CONST1/C1,C2,C3,C4,C5,C6,C7,C8,C9,Q1,Q2
COMMON/CONST2/ C10,C11,C12,C13,C14,C15,C16
COMMON/CONST5/ MODE

Z1=ACOS(1./(1.+C4/HRND-C5*ALPHND/HRND))
Z2=ACOS(1./(1.+C6/HRND+C7*ALPHND/HRND))
SINZ1=SIN(Z1)
SINZ2=SIN(Z2)
COSZ1=COS(Z1)
COSZ2=COS(Z2)
SECTH1=(C8*HRND**2+C9+Q1*SINZ1*COSZ1/2./Z1+Q2*SINZ2*COSZ2/2./Z2)/
1(SINZ1*(2.+COSZ1)*Q1/3./Z1+Q2*SINZ2*(2.+COSZ2)/3./Z2)
SECTH2=SECTH1
CON1=-C8*Z1*HRND**2/Q1-0.5*(Z1+SINZ1*COSZ1)+SECTH1/3.*(2.+COSZ1)
1*SINZ1
CON2=-0.5*(Z2+SINZ2*COSZ2)+SECTH2/3.*(2.+COSZ2)*SINZ2
IF (MODE.EQ.2) GO TO 10
C FOR RING AT BOTTOM OF THE RING GROOVE
XMOM1=C10*(1.-C11*ALPHND)**2+C2+1-C12*ALPHND-C13*ALPHND
XMOM2=C14*(1./HRND*(SINZ1/Z1+C3*SINZ2/Z2+3./Z1*(SINZ1-Z1*SECTH1/2.
1-SECTH1/4.*SIN(2.*Z1))-3./Z2*C3*(SINZ2-Z2*SECTH2/2.-SECTH2/4.*
2 SIN(2.*Z2))))*(1.-C11*ALPHND)
XMOM3=-C15/HRND**2.*((C3/Z2)**2*(Z2**2/4.+SINZ2**2/4.-SECTH2/3.*
1(SINZ2**2/2.-2.*(COSZ2-1.))+CON2*Z2)-1./Z1**2*(Z1**2/4.+SINZ1**2/4.
2-SECTH1/3.*(SINZ1**2/2.-2.*(COSZ1-1))+CON1*Z1))
XMOM4=C16/HRND**2*(1./Z1**3*(Z1**3/6.+SIN(2.*Z1)/16.-Z1/8.*COS
1(2.*Z1)+2.*SECTH1/3.*(Z1*COSZ1-SINZ1-SIN(2.*Z1)/16.+Z1*COS(2.*
2 Z1)/8.))+CON1*Z1**2/2.))+1./Z2**3.*C3**3.*(Z2**3/6.+SIN(2.*Z2)/16.
3-Z2/8.*COS(2.*Z2)+2.*SECTH2/3.*(Z2*COSZ2-SINZ2-SIN(2.*Z2)/16.
4+Z2*COS(2.*Z2)/8.))+CON2*Z2*Z2/2.))
XMOMNT=XMOM1+XMOM2+XMOM3+XMOM4
RETURN

C FOR MODE 2, WHERE RING IS AT THE TOPLAND OF THE PISTON GROOVE
10 XMOM1=-C10*(1.+C11*ALPHND)**2.+1.+C12*ALPHND-C13*ALPHND
XMOM2=-C14*(1./HRND*(SINZ1/Z1+C3*SINZ2/Z2+3./Z1*(SINZ1-Z1*SECTH1
1/2.-SECTH1/4.*SIN(2.*Z1))-3./Z2*C3*(SINZ2-Z2*SECTH2/2.-SECTH2/4.*

```

```

2SIN(2.*Z2))))*(1.-C11*ALPHND)
  XMOM3=-C16/HRND**2*((C3/Z2)**2*(Z2*Z2/4.+SINZ2**2/4.-SECTH2/3.*
1(SINZ2**2/2.-2.*(COSZ2-1.))+CON2*Z2)-1./Z1**2.*(Z1**2/4.+SINZ1**2
2/4.-SECTH1/3.*(SINZ1**2/2.-2.*(COSZ1-1.))+CON1*Z1))
  XMOM4=-C16/HRND**2*(1./Z1**3.*(Z1**3./6.+SIN(2.*Z1)/16.-Z1/8.*
1 COS(2.*Z1)+2./3.*SECTH1*(Z1*COSZ1-SINZ1-SIN(2.*Z1)/16.+Z1*COS(2.
2*Z1)/8.))+CON1*Z1**2/2.))+1./Z2**3*C3**3*(Z2**3/6.+SIN(2.*Z2)/16.
3-Z2/8.*COS(2.*Z2)+2./3.*SECTH2*(Z2*COSZ2-SINZ2-SIN(2.*Z2)/16.
4 +Z2*COS(2.*Z2)/8.))+CON2*Z2*Z2/2.))
  XMOMNT=XMOM1+XMOM2+XMOM3+XMOM4
  RETURN
  END

```

```

SUBROUTINE BISHR(HRNDA,HRNDB,EPSIL,ALPHND,C,RESIDC,IFLAG)

```

```

C-----
C      GIVEN THE TILT ANGLE, CALCULATE THE APPROPRIATE FILM HEIGHT
C      USING THE SAME BISECTION METHOD AS BISALP
C.....

```

```

C BISECTION FOR F=0 FOR FIXED ALPHND AND VARIABLE HRND

```

```

  IFLAG=1
  I=0.
  A=HRNDA
  CALL FORCE (A,ALPHND,RESIDA)
50 IF (A.GE.HRNDB)GO TO 30
  B=A+1.0
  CALL FORCE (B,ALPHND,RESIDB)

10 IF (ABS(A-B).LT.EPSIL) GO TO 60
  I=I+1
  C=(A+B)/2.
  CALL FORCE (C,ALPHND,RESIDC)
  IF ((RESIDA*RESIDB).GT.0.0) GO TO 40
  IF ((RESIDA*RESIDC).LT.0.0) GO TO 20
  A=C
  RESIDA=RESIDC
  GO TO 10

20 B=C
  RESIDB=RESIDC
  GO TO 10

40 A=B
  RESIDA=RESIDB
  GO TO 50

60 IF (C.LT.HRNDA.OR.C.GT.HRNDB) GO TO 40
  RETURN

30 WRITE (5,31) A,RESIDA,B,RESIDB,C,RESIDC
  WRITE (3,31) A,RESIDA,B,RESIDB,C,RESIDC
31 FORMAT (1X,'THE RESIDUE IN BISECTION OF HRND HAVE THE SAME SIGNS',
1/,6(1X,G10.4),I2)

```

32 FORMAT (1X,7(1X,G10.4),I2)

IFLAG=0
RETURN
END

SUBROUTINE FORCE (HRND,ALPHND,RESIDU)

```

C-----
C   FOR THE GIVEN FILM HEIGHT AND TILT ANGLE, CALCULATE THE
C   RADIAL FORCE RESIDUE
C.....
COMMON/CONST1/C1,C2,C3,C4,C5,C6,C7,C8,C9,Q1,Q2
COMMON/CONST5/ MODE

Z1=ACOS(1./(1.+C4/HRND-C5*ALPHND/HRND))
Z2=ACOS(1./(1.+C6/HRND+C7*ALPHND/HRND))
SINZ1=SIN(Z1)
COSZ1=COS(Z1)
SINZ2=SIN(Z2)
COSZ2=COS(Z2)
SECTH1=(C8*HRND**2+C9+Q1*SINZ1*COSZ1/2./Z1+Q2*SINZ2*COSZ2/2./Z2)/
1(SINZ1*(2.+COSZ1)*Q1/3./Z1+Q2*SINZ2*(2.+COSZ2)/3./Z2)
SECTH2=SECTH1
CON1=-C8*Z1*HRND**2/Q1-0.5*(Z1+SINZ1*COSZ1)+SECTH1/3.*(2.+COSZ1)
1*SINZ1
CON2=-0.5*(Z2+SINZ2*COSZ2)+SECTH2/3.*(2.+COSZ2)*SINZ2
IF (MODE.EQ.2) GO TO 13
C RING STAYS ON THE BOTTOM OF THE RING GROOVE
RESIDU=-(1.+C2)+C1/HRND**2.*((C3/Z2)**2*(Z2*Z2/4.+SINZ2**2/4.
1 -SECTH2/3.*(SINZ2**2/2.-2.*COSZ2+2.)+CON2*Z2)-1./Z1**2*(Z1*Z1/4.
2 +SINZ1**2/4.-SECTH1/3.*(SINZ1**2/2.-2.*COSZ1+2.)+CON1*Z1))
RETURN
C RING STAYS ON THE TOP OF THE RING GROOVE
13 RESIDU=-1.+C1/HRND**2.*((C3/Z2)**2*(Z2*Z2/4.+SINZ2**2/4.
1 -SECTH2/3.*(SINZ2**2/2.-2.*COSZ2+2.)+CON2*Z2)-1./Z1**2*(Z1**2
2 /4.+SINZ1**2/4.-SECTH1/3.*(SINZ1**2/2.-2.*COSZ1+2.)+CON1*Z1))
RETURN
END

```

SUBROUTINE AXIFOR(ALPHND,HRND,FMUND)

```

C-----
C   CALCULATE FOR THE AXIAL FORCE RESIDUE
C.....
COMMON/CONST3/ C17,C18,C19,C20,C21
COMMON/CONST1/C1,C2,C3,C4,C5,C6,C7,C8,C9,Q1,Q2
COMMON/CONST5/ MODE

Z1=ACOS(1./(1.+C4/HRND-C5*ALPHND/HRND))
Z2=ACOS(1./(1.+C6/HRND+C7*ALPHND/HRND))

```

```

SINZ1=SIN(Z1)
SINZ2=SIN(Z2)
COSZ1=COS(Z1)
COSZ2=COS(Z2)
SECTH1=(C8*HRND**2+C9+Q1*SINZ1*COSZ1/2./Z1+Q2*SINZ2*COSZ2/2./Z2)/
1(SINZ1*(2.+COSZ1)*Q1/3./Z1+Q2*SINZ2*(2.+COSZ2)/3./Z2)
SECTH2=SECTH1
CON1=-C8*Z1*HRND**2/Q1-0.5*(Z1+SINZ1*COSZ1)+SECTH1/3.*(2.+COSZ1)
1*SINZ1
CON2=-0.5*(Z2+SINZ2*COSZ2)+SECTH2/3.*(2.+COSZ2)*SINZ2
FMUND=-C17*SINZ1/Z1/HRND-C18*SINZ2/Z2/HRND-C17*3./Z1/HRND*
1(SINZ1-Z1*SECTH1/2.-SECTH1/4.*SIN(2.*Z1))+C18*3./Z2/HRND*
2(SINZ2-Z2*SECTH2/2.-SECTH2/4.*SIN(2.*Z2))
IF (MODE.EQ.1) GO TO 16
C. MODE=2 RING IS AT THE TOPLAND
FORCND=-FMUND+C19*(1.+C11*ALPHND)+C21
IF (FORCND.GT.0.0) GO TO 41
RETURN
41 MODE=1
RETURN
16 CONTINUE
C. MODE=1 RING IS AT THE BOTTOMLAND
FORCND=-FMUND+C19*(1.-C11*ALPHND)+C21
IF (FORCND.LE.0.0) GO TO 51
RETURN
51 MODE=2
RETURN
END

```

SUBROUTINE KINETC

```

C -----
C     CALCULATES FOR THE VELOCITY AND ACCELERATION OF THE PISTON
C     .....
COMMON // Y,DY,DDY
COMMON /KINDAT/ THTA,DTHTA,DDHTA,PHI,DPHI,DDPHI
COMMON /CRANK/ AL,R
C AL   =LENGTH OF CONNECTING ROD
C R    =CRANK RADIUS OF ROTOR
C THTA =ANGLE OF ROTOR FROM TDC OF COMBUSTION
C DTHTA =SPEED OF ROTOR
C DDHTA=ANGULAR ACCELERATION OF ROTOR
C PHI  =ANGLE OF CONNECTING RFOD RELATIVE TO CENTERLINE
C DPHI =SPEED OF CHANGE OF PHI
C DDPHI =SPEED OF CHANGE OF DPHI
C Y    =POSITION OF PISTON, COMPRESSION MOVEMENT BEING POSITIVE
C DY   =VELOCITY OF PISTON, COMPRESSION MOVEMENT BEING POSITIVE
C DDY  =ACCELERATION OF PISTON
C CALCULATE VARIABLES
STHTA=SIN(THTA)
CTHTA=COS(THTA)
RATIO=R/AL
PHI  =ASIN(RATIO*STHTA)

```

```

CPHI =COS(PHI)
SPHI =SIN (PHI)
Y     =R*CTHTA+AL*CPHI-AL+R
DPHI  =DTHTA*RATIO*CTHTA/CPHI
DY    =-(DTHTA*R*STHTA+DPHI*AL*SPHI)
DDPHI=DDTHTA*RATIO*CTHTA/CPHI+DPHI**2.*TAN(PHI)-DTHTA**2.
1     *RATIO*STHTA/CPHI
DDY   =-(DDTHTA*R*STHTA+DTHTA**2.*R*CTHTA+
1     DDPHI*AL*SPHI+DPHI**2.*AL*CPHI)
RETURN
END

```

```

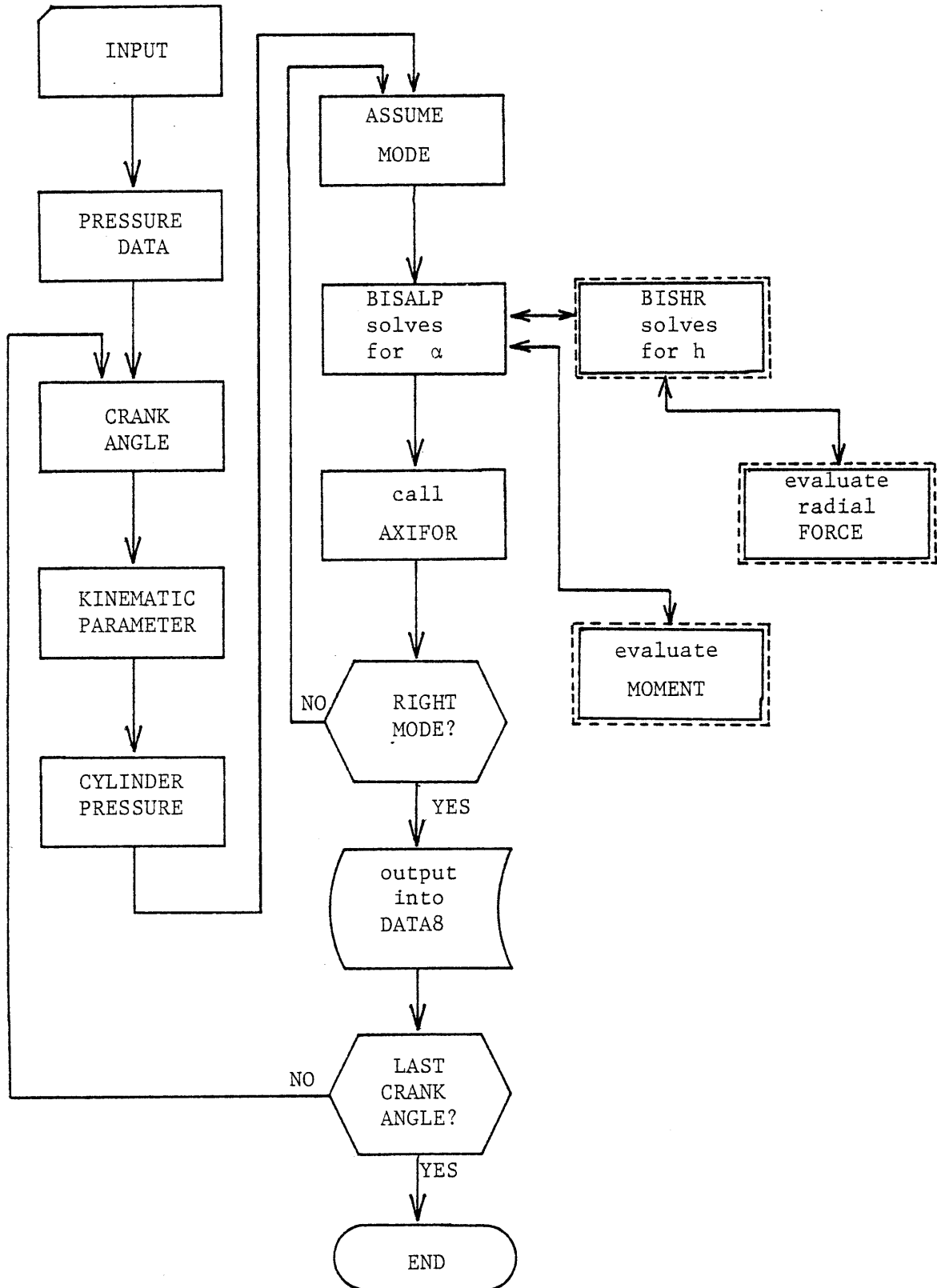
SUBROUTINE INTPOL(X2,X1,Y2,Y1,X,Y)

```

```

C-----
Y=Y1+(Y2-Y1)/(X2-X1)*(X-X1)
RETURN
END

```



APPENDIX B3: DATA7 Input Format Sample

0.2286	0.0492	3000.	7900.	2.05E11	.0033594	93539.
8.0						
4.293	1.981	0.0500	0.4846	1.981	700.	14.0
0.001						
0.001	5.	0.5	1.981000	1.981000	0.001	
004						
000.	1.					
180.	1.					
540.	1.					
720.	1.					
10.						
20.						
30.						
.						
.						
.						
690.						
700.						
710.						
0.						

0.2286	connecting rod length in m
0.0492	crank radius in m
3000.	engine rpm
7900.	ring density in Kg/m ³
2.05E11	Ring modulus of elasticity in Pa
.0033594	oil dynamic viscosity in Pa-s
93539.	ring elastic pressure in Pa
8.0	compression ratio
4.293	ring radial width in mm
1.981	ring axial width in mm
0.05	cylinder bore in m
.4846	characteristic ring tilt angle in minutes
1.981	characteristic film height in μm
700.	oil density in Kg/m ³
14.0	maximum N-D ring tilt angle
0.001	convergence criterion
0.001	minimum N-D film height
5.	maximum N-D film height
0.5	normalized position of ring profile crest
1.981	upper edge ring profile height in μm
1.981	lower edge ring profile height in μm
0.001	angle convergence criterion

APPENDIX B4: DATA8 Output Format Sample

CR Angle	ΔP (atm)	h'	α'	F_{μ}'	Y	U	accel.	mode
10.00	0.0000	0.8106	2.668	0.3223	0.9749E-01	-3.253	-5766.	2
20.00	0.0000	1.023	2.484	0.5110	0.9481E-01	-6.359	-5371.	2
30.00	0.0000	1.166	2.447	0.6557	0.9048E-01	-9.177	-4740.	2
.
.
.
170.0	0.0000	0.7266	3.137	0.2305	0.5877E-03	-2.115	3798.	1
190.0	0.7363E-02	0.7207	-3.072	-.2447	0.5877E-03	2.115	3798.	1
200.0	0.2997E-01	0.9063	-2.772	-.3978	0.2347E-02	4.214	3755.	1
210.0	0.6942E-01	1.022	-2.594	-.5325	0.5264E-02	6.279	3670.	1
220.0	0.1286	1.100	-2.457	-.6569	0.9312E-02	8.281	3524.	1
330.0	8.832	0.5449	-2.109	-1.344	0.9048E-01	9.177	-4740.	1
340.0	12.37	0.4219	-2.355	-1.168	0.9481E-01	6.359	-5371.	1
350.0	20.89	0.2598	-2.977	-.9238	0.9749E-01	3.253	-5766.	1
370.0	41.10	0.4043	13.45	0.5452	0.9749E-01	-3.253	-5766.	1
380.0	40.45	0.5332	12.98	0.8275	0.9481E-01	-6.359	-5371.	1
390.0	35.38	0.6465	12.62	1.001	0.9048E-01	-9.177	-4740.	1
400.0	27.35	0.7735	12.21	1.075	0.8469E-01	-11.59	-3915.	1
410.0	19.70	0.9082	11.57	1.090	0.7770E-01	-13.50	-2950.	1
420.0	14.54	1.020	10.68	1.092	0.6979E-01	-14.85	-1906.	1
.
.
.
710.0	0.0000	0.8047	-2.619	-.3402	0.9749E-01	3.253	-5766.	2
IMEP = 116.3	FMEP = -.6300	SFRIND = -3.283	FRICOE = -4.6434E-02					
RPM = 3000.	ALPMND =	14.00	VISCOSITY = 0.335940E-02					
0.23	0.05	3000.00	7900.00	2.05E11	0.00	93539.00	8.00	
0.00	0.00	0.05	0.00	0.00*****		14.00	0.00	
0.00	5.00	0.00	0.00	0.00	0.00			
AR = 1.084	S = 1243.	T = 1001.						
V = 0.3570	OMEGA = 0.7007							